Received: 25 August 2022 | Revised: 1 April 2023 | Accepted: 3 April 2023

DOI: 10.1002/hyp.14873

RESEARCH ARTICLE

WILEY

Spatiotemporal variability of stable isotopes in precipitation and stream water in a high elevation tropical catchment in the Central Andes of Colombia

Andrés Tangarife-Escobar[1,2] | Paul Koeniger[3] | Juan Ignacio López-Moreno[4] | Santiago Botía[1] | Jorge Luis Ceballos-Liévano[5]

[1]Department of Biogeochemical Processes, Max-Planck Institute for Biogeochemistry, Jena, Germany

[2]Technical University of Braunschweig, Braunschweig, Germany

[3]Groundwater Resources, Federal Institute for Geosciences and Natural Resources (BGR), Hannover, Germany

[4]Procesos Geo-ambientales y Cambio Global, Pyrenean Institute of Ecology, Zaragoza, Spain

[5]Subdirección de Ecosistemas e Información Ambiental, Colombian Institute for Hydrology, Meteorology and Environmental Studies (IDEAM), Bogotá, Colombia

Correspondence
Andrés Tangarife-Escobar, Max Planck Institute for Biogeochemistry, Hans-Knöll-Straße 10 07745 Jena, Germany.
Email: atanga@bgc-jena.mpg.de

Funding information
Deutscher Akademischer Austauschdienst; MARGISNOW (Spanish Ministry of Science and Innovation), Grant/Award Number: PID2021-124220OB-100

Abstract

The Colombian Andean Mountains include the headwaters of the main basins of the country. However, the isotope composition of water in these high mountain ecosystems has been poorly studied. In this study, we analysed the first set of stable isotope data collected along a wide elevation range (2600–4950 m a.s.l.) in the Central Andes of Colombia. The stable isotope composition of stream water and precipitation was determined for a period between 2017 and 2018 in the Upper Claro River basin. The driving factors influencing the spatial and temporal variability of δ^2H, $\delta^{18}O$, and d-excess were identified, and compared with daily air temperature and precipitation data from seven meteorological stations. The local regression line was described by $\delta^2H = 8.2\ \delta^{18}O + 12.3$, $R^2 = 0.98$. The δ^2H and $\delta^{18}O$ values showed more depletion in heavy isotopes, and the d-excess values were more negative during the rainy season. An altitude effect of −0.11‰/100 m and −0.18‰/100 m was estimated for stream water and precipitation $\delta^{18}O$ values, respectively, with the latter showing non-linear behaviour. The dataset was compared with Colombian stations of the Global Network of Isotopes in Precipitation database, and a back-trajectory analysis of air masses was conducted and compared with the d-excess values. The $\delta^{18}O$ weighted mean values changed with respect to the position in the Central Andes, indicating contrasting altitude effects depending on the moisture sources. The most positive d-excess values were attributed to moisture recycling enhanced by local ecosystem conditions and the origin of precipitation from the Amazon basin, which change during the year and across the northern Andes. The results showed a high level of variation because of differences in elevation, seasonality, and atmospheric circulation patterns during the year. This study contributes to knowledge of spatial and temporal isotope composition data in the northern Andes, delineation of water supply basins, and to the definition of ecosystem boundaries in the high mountains of Colombia.

KEYWORDS
air mass back-trajectory, altitude effect, Colombian Andes, d-excess, northern Andes, seasonal effect, stable isotopes

1 | INTRODUCTION

The interaction between environmental factors and the water cycle has been of increasing concern during recent decades. Climate change and anthropogenic factors are posing threats to water availability on local and global scales (IPBES, 2019; IPCC, 2022). The analysis of the stable isotopes in water (deuterium: ^{2}H; oxygen-18: ^{18}O) is essential to enable understanding of the factors affecting hydrological processes, and consequently the impacts of environmental change on local and regional moisture sources and water recharge areas. Understanding of the complex relationships between isotope signatures and meteorological, hydrological, geological, and land cover characteristics is particularly important in high elevation catchments including in the northern Andes, encompassing Ecuador, Colombia, and Venezuela. In this area water availability strongly depends on stream water from high mountain ecosystems including glaciers, páramos, cloud forest, and Andean forest (Buytaert et al., 2006; Escobar et al., 2022; Harden et al., 2013; Rodríguez-Morales et al., 2019).

Because of their relevance to the water cycle, páramo ecosystems have been widely studied (Hofstede, 2003; Sarmiento et al., 2013; Sklenar et al., 2010; van der Hammen & Cleef, 1986). The Andean páramos comprise a large variety of lakes, peat bogs, and wet grasslands where the soil can be up to several meters thick (Buytaert et al., 2006). In these environments the cold and wet conditions have favoured organic matter accumulation, which along with the input of volcanic ash has resulted in organic soils having porous structure (Buytaert et al., 2005), high water retention, and high hydraulic conductivity (Nanzyo et al., 1993; Rousseaux & Warkentin, 1976; Shoji & Fujiwara, 1984;). Páramos are known to have higher levels of precipitation than runoff and evapotranspiration (Buytaert, 2004); this is reflected in a sustained base flow and extreme water regulation capacity (Hofstede, 1995; Luteyn, 1992; Podwojewski et al., 2002; Poulenard et al., 2003). However, despite the importance of these ecosystems for Colombia, stable isotope investigations in páramos have been mainly conducted in Ecuador, Bolivia, and Perú (Bershaw et al., 2016; Fiorella et al., 2015; Valdivielso et al., 2020).

The spatial and temporal distribution of $\delta^{2}H$ and $\delta^{18}O$ isotopes in South America has been related to four main factors (Rozanski & Araguas-Araguas, 1995) including: (1) water input from three atmospheric moisture sources (the Atlantic and Pacific oceans and the Caribbean Sea); (2) the Andes Mountains blocking free air flow and leading to enhanced condensation along the slopes; (3) the proximity of the world's largest source of continental evapotranspiration (the Amazon Basin); and (4) the seasonal movement of the Intertropical Convergence Zone (ITCZ). The Amazon rainforest contributes large amounts of recycled moisture to the air masses transported by trade winds (Ampuero et al., 2020; Martinelli et al., 1996; Vallet-Coulomb et al., 2008). These conditions (mainly temperature and vapour, but also topographical conditions) determine the stable water isotope patterns in the hydrological cycle. Precipitation effects (including continental, seasonal, and altitude effects) cause predictable stable isotope compositions for local sites, landscapes, and regions. Additionally, a second order isotope parameter, termed deuterium excess (d-excess; $=\delta^{2}H\text{-}8\ \delta^{18}O$; Dansgaard, 1964), represents the *y*-intercept from the Global Meteoric Water Line (GMWL) (Bershaw et al., 2020; Gonfiantini, 1998), and characterizes the non-equilibrium fractioning during evaporation in the source area, temperature of condensation, and the degree of moisture recycling (Froehlich et al., 2008; Jouzel & Merlivat, 1984; Liotta et al., 2006; Rank & Papesch, 2005). On a global basis, relative humidity, sea surface temperature, and wind speed are the main controlling parameters (Benetti et al., 2014; Clark & Fritz, 1997; Rozanski et al., 1993).

Consistent with these factors, regional models of stable isotopes in precipitation over the tropical Americas have shown that variations in precipitation depend on both local meteorological factors and the interaction of several regional patterns, mainly the El Niño Southern Oscillation (ENSO) and the South American Summer Monsoon (SASM) (Vimeux et al., 2005; Vuille et al., 2003, 2012; Vuille & Werner, 2005). In the tropical Andes specifically, atmospheric circulation patterns varying in direction during the austral winter and austral summer also influence the isotope composition of atmospheric water vapour (Samuels-Crow et al., 2014; Villacis et al., 2008). For example, it has been suggested that stable isotope values for snow in the austral summer in the Peruvian Andes reflect regional-scale atmospheric forcing, but during the austral winter they are modulated by temperature, heating related to topography, or wind regimes on the ice cap surface (Hurley et al., 2015).

The spatial variability in isotope composition in the equatorial region is also dominated by the altitude effect. The $\delta^{18}O$ composition in precipitation changes with elevation at a rate of −0.2‰/100 m (up to 3000 m a.s.l.), and declines above 3000 m a.s.l. to −0.5‰/100 m (Rozanski & Araguas-Araguas, 1995). A similar effect has also been observed for stream waters, where the isotope composition is generally modified by surface water mixing and/or evaporation (Bershaw et al., 2016). In high mountain ecosystems, including the páramos of Costa Rica and Ecuador, the isotope composition in precipitation has been found to be influenced by Amazon rainforest air masses during passage of the ITCZ in wetter seasons, and by orographic precipitation during the transition and drier seasons (Esquivel-Hernández et al., 2019).

In the Colombian Andes there is an absence of continuous and well-distributed stable isotope data, and the driving factors affecting stable isotope composition are still poorly understood. Only 11% (four) of the stations available in the Global Network of Isotopes in Precipitation (GNIP) have samples for at least five consecutive years (60 samples) been collected, and only one includes data up to 2021.

Stable isotope data have been commonly collected during time-limited campaigns, and consulting projects where data acquisition terminates with the cessation of funding. In most cases the data have remained unpublished (Vuille, 2018). Several stable isotopes studies have been conducted in different hydrological systems and using various investigative techniques. Based on 800 samples from a number of studies, Rodríguez (2004) developed a local meteoric water line (LMWL) equation for Colombia: $\delta^2H = (8.03 \pm 0.28)\ \delta^{18}O + 9.6$, and reported that the δ-values during the dry season were higher than during the rainy season, and that they were more enriched near the oceans than in the inner part of the country, because of the lower elevation and proximity to the coast. The lowest δ-values did not coincide with the highest precipitation rates, which was explained by the various sources of rain fronts affecting the central part of the country (the Atlantic Ocean through either the Amazon basin or the Caribbean, and the Pacific Ocean).

Other stable isotope studies focused on groundwater exploitation in Colombia have mainly focused on the identification of recharge areas and residence times in the Eastern Andes (Castrillon et al., 2003; Mariño-Martinez et al., 2018); the Caribbean region (Campillo et al., 2021; Toro et al., 2009); the Cauca River (Betancur & Palacio, 2007; Medina et al., 2009), and the areas surrounding the Upper Claro River basin (UCRB) (Otálvaro et al., 2009). For instance, Saylor et al. (2009) found that the precipitation amount exerts the greatest effect on $\delta^{18}O$ and δ^2H at the GNIP stations in the vicinity of Bogotá. Nonetheless, the scope of these studies has been spatially and temporarily limited, and studies directed at understanding the driving factors that affect the stable isotope composition across the complex orography and climatic setting of the country have not yet been undertaken. In this report we provide the first stable isotope dataset for the area, derived by the Colombian Institute for Hydrology, Meteorology and Environmental Studies (IDEAM), as a contribution to the study of high mountain ecosystems highly threatened by environmental and anthropogenic change.

The dataset enabled analysis of spatiotemporal variations in the isotope composition of stream water and precipitation in the UCRB. For this purpose the leading questions were: (i) how did the stable isotope values for precipitation and stream water vary in the UCRB over the period (2017–2018); (ii) how did the stable isotope composition vary as a function of elevation in the UCRB, and how was this related to other geographical regions of the country; and (iii) what were the main sources of precipitation during the 2017–2018 period in the UCRB, and how are moisture sources and land cover characteristics of the northern Andes related to the observed isotope patterns?

2 | MATERIALS AND METHODS

2.1 | Location and climate of the Upper Claro River basin

Colombia is located in the northwest of South America, and its land area extends to the Caribbean Sea in the north, the Pacific Ocean in the west, and the Amazon rainforest in the south. Three mountain ranges dominate the topography, including the Western, Eastern, and Central Cordilleras (Figures 1 and 2). The UCRB is a high elevation tropical catchment (65 km^2) in the Colombian Central Andes. It extends topographically from 2600 to 4995 m a.s.l., and provides water for industry, agriculture, and human consumption over a large area. There are seven meteorological stations in the basin over an elevation range of 2714–4699 m a.s.l. (Figure 2), and these are used to study the short hydrological response of the Conejeras glacier at the summit of the UCRB (Ceballos et al., 2006; Morán-Tejeda et al., 2018) (Table 1). Mölg et al. (2017) have reported that this tropical glacier (0.2 km^2) is important in recording and understanding climate variability, as it plays a major role in modulating the arrival of water from the summit areas to the páramo (Morán-Tejeda et al., 2018), despite comprising only 1.3% of the watershed (WGMS, 2017). However, we were not able to investigate the effect of this glacier on the isotope composition, as snow accumulation on the glacier takes place over very short periods, and the snowmelt water resulting from thaw of the permanent glacier is always mixed with precipitation in the form of runoff (as found by analyzing the water at river water station S5, which was situated at the outlet of the Conejeras glacier).

The Nevado del Ruiz volcano (NRV) and Nevado de Santa Isabel volcano (NSIV) limit the upper basin at the top of the UCRB. They contribute to the hydrothermal and volcanic activity of the region (Bohórquez et al., 2005; Robertson et al., 2002), which influences the UCRB through a hot spring that actively contributes water to the basin. Geothermal and geological studies have described a complex tectonic system composed of faults, fractures, and unconformities that configure a network of shallow and deep-water circulation systems in the UCRB and across wider areas of the Central Colombian Andes (Arango et al., 1970).

The climate in the northern Andes is defined by topographic factors, but also by the meridional displacement of the ITCZ and ENSO phenomenon (Arias et al., 2015; Hastenrath, 2002; Sakamoto et al., 2011). Trade winds from the Atlantic and Pacific oceans and the Amazon forest, and a surface tropical westerly termed the Chocó Stream all affect the local meteorology (Poveda et al., 2006). The weather follows a bimodal regime involving two rainy and two dry seasons. Although precipitation occurs in the UCRB throughout the year, suggesting the absence of a strictly dry season, there is a clear contrast between months associated with continuous rain events, and months having less rain; here we refer to the latter as the dry period or season. The rainy periods occur from March to May (MAM) and September to November (SON), with the monthly average being higher for the latter period. The dry periods are from June to August (JJA) and December to February (DJF) (Rabatel et al., 2018). The annual average precipitation is 1300 mm, the environmental lapse rate is −0.52°C/100 m, and the average relative humidity is 83% for the entire basin (Peña, 2016). In the highest areas the mean temperature is −2 to 4°C (WGMS, 2017). The annual evapotranspiration is 300–500 mm (Ocampo-López, 2012), with the highest values in DJF (52 mm) and the lowest in February and September (45 mm); the evapotranspiration decreases with increasing elevation.

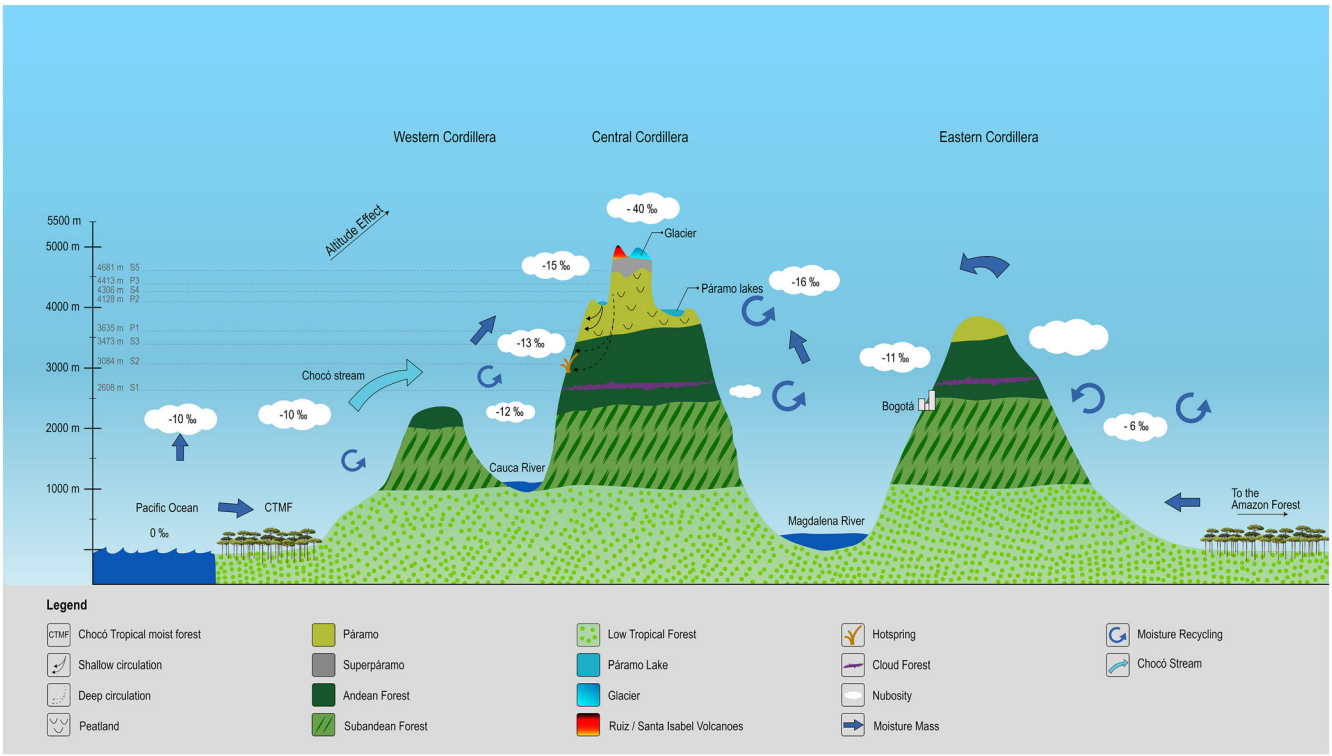

FIGURE 1 Cross section (A-B; N45°W–S45°E; see Figure 2) across the three branches of the northern Andes in Colombia, showing the main features influencing the water cycle of the Upper Claro River Basin (UCRB). This illustrates the relationship between air trajectories and stable isotope composition in precipitation. In the west, the Pacific Ocean waters evaporate and travel to the east along the main wind direction, and generate one of the rainiest areas of the world on the Chocó Tropical Moist Forest (CTMF) and the western flank of the Western Colombian Andes (7000–9000 mm/year; IDEAM, 2011). Air masses reach the highest elevations of the UCRB helped by the Choco Stream following several moisture recycling events, and as $\delta^{18}O$ and $\delta^{2}H$ deplete with altitude and increased continentality. In the east, the Atlantic Ocean waters evaporate and travel to the west, crossing the Amazon Forest after several moisture recycling events. When vapour reaches the Andes it forms a high precipitation belt on the eastern flank of the Eastern Colombian Andes (5000–7000 mm/year; IDEAM, 2011). In the UCRB, four main ecosystems occur with increasing elevation (Andean forest, cloud forest, páramo, and glacier). The páramo is characterized by an abundance of lakes, wetlands, and peatlands. The páramo ecosystem has been formally divided into subpáramo, páramo, and superpáramo. For simplification the subpáramo is not shown (Illustration by María Camila Botía, @mariabotia11).

Based on studies of wind directions and the sources of moisture (Hoyos et al., 2018; IDEAM & UPME, 2017), the Central Andes of Colombia are a convergent area for air masses throughout the year. During the first rainy season (MAM), the inter-Andean region shows moisture convergence and the main wind directions are from the southeast and west. In contrast, during the second rainy season (SON) the main wind directions are from the northeast and west (Pacific Ocean). At the beginning of the first dry season (DJF) the main wind directions are from the north and west, with additional inputs from the southeast, while in the second dry season (JJA) the main wind directions are from the south and west.

2.2 | Data collection and analysis

We integrated meteorological data (air temperature and precipitation 2 m above ground) with the water composition of stable isotopes. Stream and precipitation water samples were periodically collected from January 2017–October 2018 from three rainfall collectors (P1: 3635 m a.s.l.; P2: 4128 m a.s.l.; and P3: 4413 m a.s.l.) and five stream sites (S1, S2, S3, S4, and S5) (Figure 3; Table 2 and Table 3). The sampling was planned to occur monthly, but for logistical reasons this was not always achieved, and consequently our analyses were constrained by the actual sampling intervals. Each precipitation collector consisted of 0.5 L glass Erlenmeyer flasks fitted with a circular funnel (0.1 m diameter) containing a plastic sieve inside to prevent contamination with debris. The flasks were placed on flat ground, and surrounding vegetation was removed to avoid interference with incoming precipitation. Stream water samples (snapshot) were manually collected using a beaker from the middle of the stream to avoid the influence of bank vegetation. Following collection, samples were transferred to 50 mL brown glass vials closed with silicone septa caps, and stored in cooling boxes until laboratory analysis. In total 140 samples were collected for $\delta^{18}O$ and $\delta^{2}H$ analysis, comprising 49 samples of precipitation and 91 samples of river water. The samples were analysed at the Stable Isotopes Laboratory of the Colombian Geological Survey (SGC) using an Off Axis Integrated Cavity Output Spectrometer (OA-ICOS) (DTL 100; Los Gatos Research). The stable isotope values of

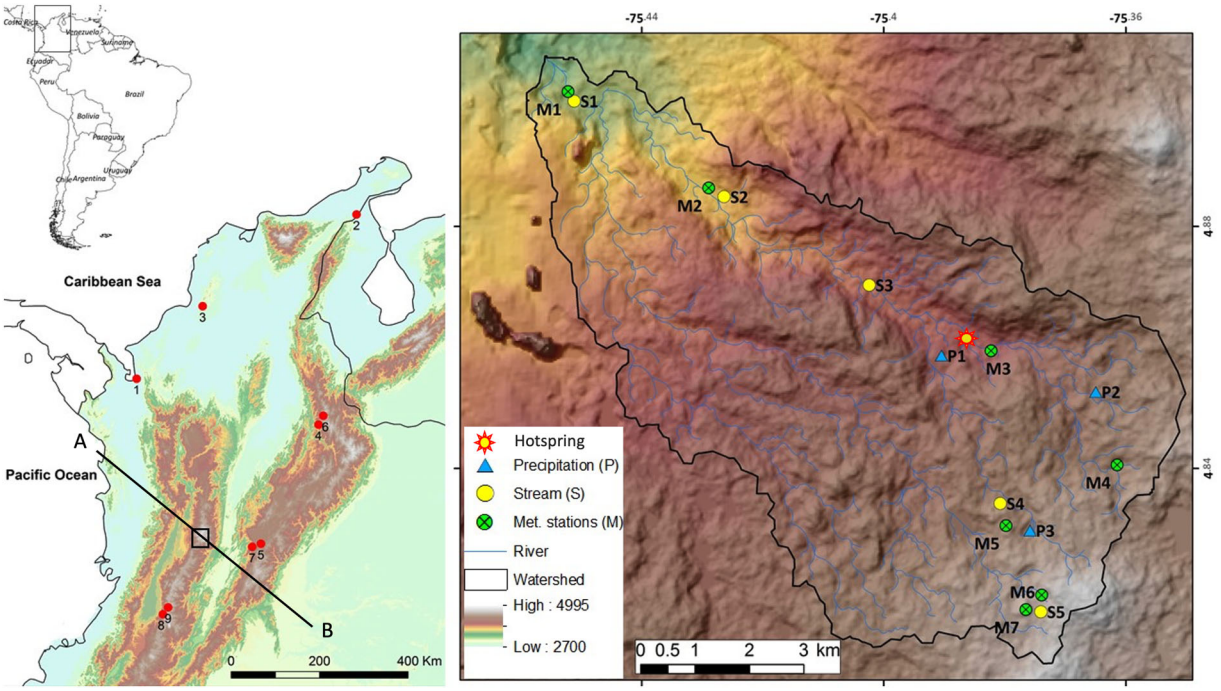

FIGURE 2 Location of the Upper Claro River Basin (UCRB) in the middle part of the Colombian Central Andes showing stream (S) and precipitation (P) sampling locations, and meteorological stations (M). Upper left: geographical position of Colombia in South America. Lower left: location of GNIP stations in Colombia. 1. Tulenapa, 2. Maicao, 3. El Tesoro, 4. La Galvicia, 5. Bogotá, 6. Tona, 7. El Hato, 8. La María, 9. Albania.

laboratory standards were calibrated against Vienna Standard Mean Ocean Water (VSMOW2) and Vienna Standard Light Antarctic Precipitation (SLAP2), and used for all measurements. All results were expressed in per mil (‰) using the conventional delta-notation relative to Vienna Standard Mean Ocean Water (V-SMOW). All plots are presented with the Global Meteoric Water Line (GMWL) defined as $\delta^2H = 8 \cdot {}^{18}O + 10$ (Craig, 1961). The analytical precision (the standard deviation of a quality check sample measured in each run) was better than 0.3‰ for $\delta^{18}O$ values and 0.8‰ for δ^2H.

To estimate any altitude effects on river water we used the mean catchment elevation, calculated using ArcGIS. Two different approaches were considered to calculate variation in the rate of $\delta^{18}O$ as a function of the elevation of the river water. In the first approach a monthly mean $\delta^{18}O$ value, derived only from samples taken simultaneously at the five stations, was used to reduce the bias resulting from seasonality effects and irregular sampling periodicity, while in the second approach all samples were considered. In both approaches the gradients were calculated from the slope of the regression lines. For precipitation, the gradient was estimated using a linear regression calculated from the precipitation-weighted (PW) mean values for each station. Hence, 24, 12, and 13 samples were considered for collectors P1, P2, and P3, respectively, because of irregularities in the sampling campaign. No precipitation was recorded at meteorological station M7, and therefore precipitation values for this station were based on data from nearby stations (M5 in 2017, and M6 in 2018). For station M1 the temperature and precipitation data from 1 January 2017 to 11 November 2017 were derived from station M2. The temperature for the sampling intervals was calculated as the average of the mean daily temperature values. Accumulated precipitation values were acquired by summing the daily amounts for the periods between samples.

The GNIP stations Tulenapa, Maicao, Albania, and Bogotá were used for regression line (RL) comparisons with data from P1, P2, and P3. Additionally, the average $\delta^{18}O$ values for the stations El Hato, La Galvicia, Tona, La Maria, and El Tesoro were downloaded to analyse elevation effects. Data were accessed on 15 June 2019 from the IAEA/WMO database (IAEA/WMO, 2020). The RL for stream water was calculated using the Ordinary Least Squares Regression (OLSR) method, which has been widely used to determine correlations between δ^2H and $\delta^{18}O$ in precipitation (Payne, 1992); this gives equal weighting to all data points regardless of their respective precipitation amounts (Crawford et al., 2014). The RL for precipitation was calculated based on the precipitation-weighted least square regression (PWLSR) approach, using the open software Local Meteoric Water Line freeware (Hughes & Crawford, 2012); this reduced the effect of small precipitation volumes and potential evaporation during sampling.

2.3 | Back-trajectory cluster analysis

To better understand the origin of the air masses arriving at our sampling sites we used the Stochastic Time Inverted Lagrangian Transport (STILT) model (Lin et al., 2003). The model was driven by 3-hourly meteorological fields from ECMWF short-term forecasts (following the contemporary IFS cycle development; more information

TABLE 1 Location and elevation of the seven Upper Claro River basin (UCRB) meteorological stations designated in this study (M), and their official names according to IDEAM (Attrib. M-stations).

Station	Region of the country	Longitude (°W)	Latitude (°N)	Elevation (m a.s.l.)	Attrib. M-stations	Period	# samples	$d^{18}O$[a] (‰ VSMOW)	SD	$d^{2}H$[a] (‰ VSMOW)	SD	DE[a] (‰ VSMOW)
P1	West	75.39050	4.85860	3635	M3	May 2017–October 2018	24	−13.44	4.07	−98.12	33.71	9.4
P2	West	75.36500	4.85260	4128	M4	July 2017–September 2018	12	−13.23	3.07	−95.54	28.10	10.3
P3	West	75.37580	4.82970	4413	M5	July 2017–October 2018	13	−15.09	3.01	−108.91	24.17	11.81
GNIP												
1. Tulenapa	Caribbean	76.65085	7.78986	30		February 2013–December 2016	46	−6.24	2.74	−39.8	22	10.1
2. Maicao	Caribbean	72.24742	11.37261	45		January 2004–September 2004	5	−5.6	3.36	−36.8	27.5	6.7
3. El Tesoro	Caribbean	74.13000	4.70000	198		January 2005–November 2016	136	−5.88	2.87	−38.3	22.11	8.7
4. La Galvicia	East	73.06000	7.12556	1848		January 2005–September 2005	9	−7.36	3.37	−45.9	28.87	13
5. Bogotá	East	74.13000	4.70000	2547		August 1971–December 2016	289	−10.56	4.33	−74	35.65	10.5
6. Tona	East	72.97389	7.19861	2660		January 2005–September 2005	9	−8.61	3.1	−58.3	26.63	10.6
7. El Hato	East	74.29086	4.50135	3150		January 1999–October 1999	10	−11.55	2.85	−80	22.05	12.4
8. La María	West	76.08044	3.30144	2100		March 2003–December 2003	9	−12.09	2.77	−87.4	23.98	9.4
9. Albania	West	76.00170	3.44052	3000		March 2003–December 2003	10	−13.09	3.41	−95.4	26.3	9.3

[a]Weighted mean.

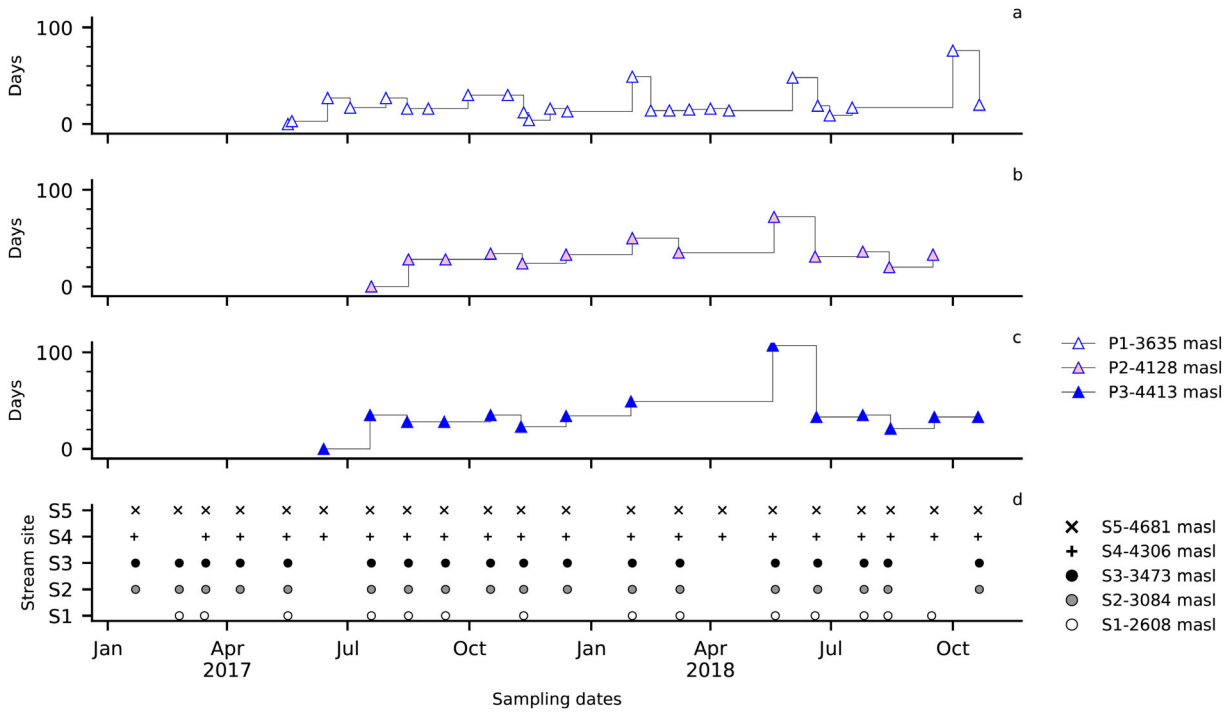

FIGURE 3 Sampling dates over the entire sampling period for cumulative rainwater at the precipitation sites (a–c), and the snapshot sampling at the stream water sites (d). The cumulative sampling at the precipitation sites commenced on the date the rain gauge was installed. The *y*-axis shows how many days passed between sampling occasions.

is available at https://www.ecmwf.int/en/publications/ifs-documentation). The IFS fields were preprocessed and interpolated to a spatial resolution of 0.25° × 0.25°. At every release time (00:00, 06:00, 12:00, 18:00) for each day throughout the period January 2017 to October 2018, a 100-particle ensemble (interpreted as an air parcel) was released at each of three representative elevations: 3600 m a.s.l. (4.8586° N, 75.3924° W; station P1); 3900 m a.s.l. (4.8501°N, 75.3924°W); and 4400 m a.s.l. (4.8297N, 75.3758° W) m a.s.l. For each release time and elevation, back-trajectories were calculated for each ensemble member for the preceding 7 days, based on the study by Ampuero et al. (2020), in which this time was considered sufficient for the back-trajectories to travel back to the point of last saturation (Hurley et al., 2012).

Based on the 100-particle ensemble, a mean back-trajectory was obtained for each release time and elevation. These were then grouped in clusters based on the time window between the collection of the precipitation samples. For example, if the rain sampler was placed on 15 May 2017 and collected on 20 May 2017 (5 days later), the cluster would contain the back-trajectories associated with May 15 and the days in between up to May 20. To create the clusters, we used the trajCluster function provided by the Openair package in R, developed by Carslaw and Ropkins (2012). We used four clusters with the 'Angle' clustering option, which groups the back-trajectories based on their arrival angle to the release location. The clusters were generated in R and then plotted in Python. The resulting clusters on coincident dates were used to interpret the d-excess signals for P1, P2, and P3. The remaining clusters for each elevation are shown as supplementary information.

3 | RESULTS

3.1 | Seasonality in stable isotope composition

Seasonal variation in the stable isotope composition of precipitation and stream water over the air temperature and precipitation variation of M3 is shown in Figure 4. During the observation period from 2017 to 2018, the isotope values for $\delta^{18}O$ and $\delta^{2}H$ in precipitation ranged from −19.89 to −2.41‰ and − 150.4 to −5.2‰, respectively, and d-excess values ranged from −4.9 to 23.8‰. For river water the stable isotope values ranged from −23.77 to −8.57‰ and − 165.5 to −61.8‰ for $\delta^{18}O$ and $\delta^{2}H$, respectively.

The isotopic values in precipitation showed wide variability, especially for P1 where the range for $\delta^{18}O$ was −19.00 to −2.41‰. However, the most depleted $\delta^{18}O$ values were found for P3 and P2 (−19.89 and − 19.42‰, respectively). At all stations more enriched values were found during dry periods (January, March, and August), while more depleted isotope values were found during the rainiest months (May and June). Most negative precipitation-weighted mean values for d-excess mainly coincided with drier periods including January, November, and a dry interval in May 2017 (P1; −4.9‰), while the most positive values occurred in February (P2; 23.8‰) and July.

Among the stream water stations the most depleted $\delta^{18}O$ values were measured at S5 in the rainy period in May 2017 (−23.77‰). This occurred 7 days after the highest daily precipitation occurred over the study period (31.6 mm, May 2017). The most enriched values were found for January 2017 (−8.57‰), following one of the driest periods of the year (precipitation did not exceed 2.3 mm/day). Stations S1, S2,

TABLE 2 Characteristics of the precipitation stations in the UCRB (this study) and international stations (derived from GNIP).

Station	Longitude (°W)	Latitude (°N)	Elevation (m a. s.l.)	Drainage ecosystem	Attrib. M-stations	Period	# samples	$d^{18}O^a$ (‰ VSMOW)	SD	d^2H^a (‰ VSMOW)	SD	DE^a (‰ VSMOW)
S1	75.4511	4.9007	2608–4947	Andean Forest > Páramo > Glacier	M1, M2	February 2017–September 2018	14	−13.23	1.49	−13.05	9.77	11.36
S2	75.4263	4.8849	3084–3276	Andean Forest	M2	January 2017– October 2018	18	−13.51	1.17	−13.55	2.72	12.58
S3	75.4024	4.8704	3473–4947	Páramo > Andean Forest	M3	January 2017–October 2018	18	−14.50	0.82	−14.60	3.36	13.11
S4	75.3807	4.8342	4306–4947	Páramo	M5	January 2017–October 2018	20	−14.18	2.83	−14.48	16.46	10.99
S5	75.3744	4.8163	4681–4947	Glacier	M5, M6, M7	January 2017–October 2018	21	−14.37	3.12	−14.94	19.25	12.00

[a]Arithmetic mean.

and S3 showed low variability in isotope values, with no clear pattern during the sampling period. Generally, d-excess values ranged from −10.8‰ (dry period) to 25.6‰ (rainy period). Interestingly, S1 showed a decrease from 25.6‰ in February to 3.7‰ in May, which corresponded to an increase in the accumulated precipitation.

Meteorological data from the UCRB showed that there were no dry periods, but rather months having fewer rainy days and less precipitation. Unfortunately, solid precipitation events were not registered at the meteorological stations. Mean daily air temperature did not have a major effect on the isotope composition, as it was relatively constant throughout the year at all meteorological stations (variations of <4°C during the study period). Comparisons of the accumulated precipitation for each sampling period with the $\delta^{18}O$ and d-excess values were conducted for all samples (Figure S1), but these comparisons were not describing the amount effect as the sample collection period included several rainfall events, and therefore the isotope signature included a mixture of low and high rain events. The correlation coefficients (R) were generally <0.6. There was also wide variation in $\delta^{18}O$ values as a function of the mean daily air temperature, and there was no clear correlation when individual precipitation samples were analyzed (Figure S1). The correlation coefficients (R values) for P1, P2, and P3 were −0.05, −0.26, and −0.31, respectively ($p > 0.1$ in all cases). For d-excess the correlation coefficients were −0.53 ($p < 0.1$) for P1, −0.08 ($p > 0.1$) for P2, and −0.22 ($p > 0.1$) for P3. Thus, only for precipitation samples from station P1 was temperature correlated with the isotope composition and d-excess.

3.2 | Altitude effect

An elevation effect on the stable isotope composition was found for precipitation and stream water (Figure 5a,b). The weighted mean values for $\delta^{18}O$ in precipitation were −13.44‰, −13.23‰, and −15.09‰ for P1, P2, and P3, respectively. The lowest station (P1) was more depleted in $\delta^{18}O$ than P2, causing a non-continuous gradient which led to an inverse tendency between P1 and P2. Overall, an altitude effect of −0.18‰ for $\delta^{18}O$/100 m was calculated ($R = -0.71$, $p > 0.1$), which indicates that the slope was not different from zero. In stream water the $\delta^{18}O$ values were generally more depleted with increasing mean catchment elevation. An average elevation effect of −0.07‰ for $\delta^{18}O$/100 m was calculated for all the stream samples taken in each station ($R = -0.16$, $p > 0.1$), which indicates that the slope was not significantly different from zero (all months in Figure 5b). Using only the months corresponding to the five stations (selected months in Figure 5b), a gradient of −0.11‰/100 m ($R = -0.79$, $p > 0.1$) was calculated based on the arithmetic average.

3.3 | d-Excess in precipitation and origin of air masses

The relationship between d-excess and elevation for precipitation samples is shown in Figure 5c. This shows two linear correlations, the

TABLE 3 Characteristics of the river water stations in the Upper Claro River basin (UCRB).

Station	Longitude (°W)	Latitude (°N)	Elevation (m a.s.l.)	Attrib. M-stations	Frequency of measurements and remarks
M1	75.45083	4.90083	2714	Rio Claro	Precipitation: daily complemented from M2
					Temperature: daily taken from M2
M2	75.42889	4.88639	3064	San Antonio	Precipitation and temperature: daily
M3	75.38222	4.85944	3637	Parque Nacional los Nevados	Precipitation and temperature: daily
M4	75.36139	4.84056	4325	Laguna Verde	Precipitation and temperature: daily
M5	75.37583	4.82972	4413	Páramo de Conejeras	Precipitation and temperature: daily
M6	75.37389	4.81750	4686	Nevado Santa Isabel	Precipitation: daily
M7	75.37444	4.81639	4699	Conejeras 2	Temperature: daily
					Precipitation: daily composed by M5 and M6

Note: Drainage ecosystems for each station are shown in order of drainage area.

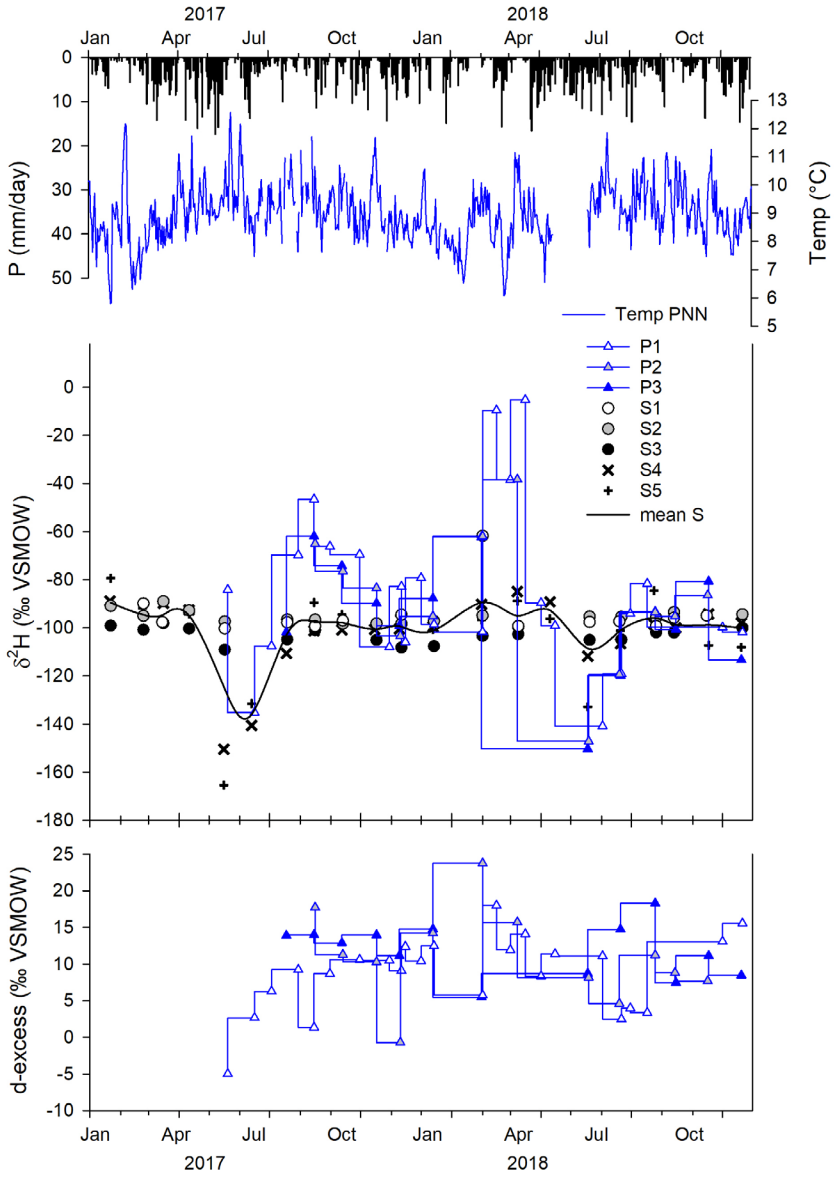

FIGURE 4 Variation of δ^2H values for the stream water (S1–S5) and precipitation (P1–P3) stations, and for d-excess (only for precipitation), compared with daily accumulated precipitation and daily mean air temperature at meteorological station M3 (PNN; 3637 m a.s.l.). Values for the period 1 January 2017 to 1 November 2018. Mean isotope values for stream samples are also shown.

first calculated based on the precipitation-weighted d-excess values and the second without weighting as a function of precipitation amount. Both regressions showed an increase in d-excess with increasing elevation, with the unweighted d-excess values (gradient of 0.43‰/100 m, $R = 0.28$, $p < 0.1$) having a slope significantly different from zero. The precipitation-weighted mean d-excess values were

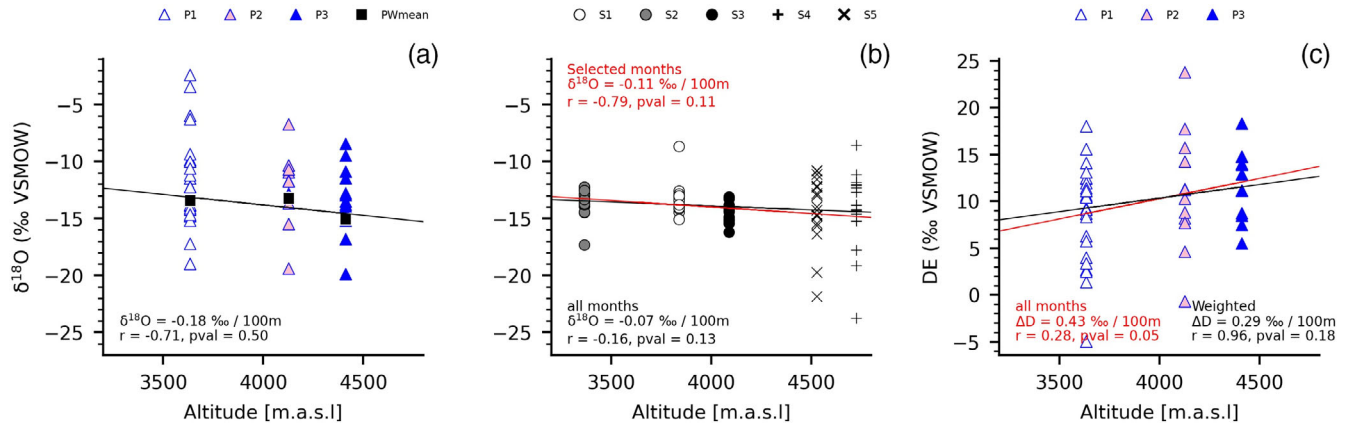

FIGURE 5 (a) Gradient of $\delta^{18}O$ values with elevation for all precipitation samples. The gradient line was calculated based on the precipitation-weighted mean value for each station (black square). (b) Gradient of $\delta^{18}O$ values with elevation for all stream water samples for months coinciding for all stations (red line) and for all sampling months (black line). (c) Relationship between elevation and d-excess values for weighted (black line) and unweighted (red line) precipitation. Elevation was calculated as the mean catchment elevation.

9.4‰, 10.3‰, and 11.8‰ for P1, P2, and P3 respectively; these values are consistent with the precipitation-weighted global average value of 11.27 (±0.65) (Rozanski et al., 1993).

As d-excess changed with elevation, we performed a back-trajectory analysis for each precipitation sampling elevation. The back-trajectory cluster analysis indicated that during the data collection period there was a consistent influence from the northern part of the Amazon basin (Figure 6, lower panel). We observed that during the boreal summer (JJA) the trajectories showed a sustained eastward direction, which sometimes extended as far as the Atlantic Ocean. During this time there was a slight influence from the south into P2 and P3, but the cluster only represented 4.4% (P2) and 6% (P3) of the ensemble. During the boreal winter (mainly DJF), the clusters showed variations in the trajectory directions with respect to the summer season. At P1 in November 2017, 43.8% of the trajectories arrived from the northeast, travelling across the Orinoco basin, and the northeastern part of the Amazon basin. The other trajectories arrived from the southwest, but had a prior influence from the western part of the Amazon basin. At P2 and P3 the clusters were very similar, with a large percentage of air masses coming from the east. In December 2017 and February 2018, the clusters at all heights had similar directions, with large contributions from the northern part of the Amazon, and one cluster (representing 19%–23% of the total ensemble) showing influences from the north (the Panama isthmus). Even though the origin of the trajectories was consistent among elevations, we conclude that P1 was markedly different from P2 and P3 in some months (e.g., August and December 2017).

3.4 | Local and regional comparisons of $\delta^{18}O$ and RLs

A comparison between precipitation-weighted $\delta^{18}O$ values and the elevations of stations in Colombia is presented in Figure 7 and Table 2. More depleted $\delta^{18}O$ values were observed with increasing elevation. A regression between $\delta^{18}O$ and elevation (only for samples located at the Andes mountains) showed a strong relationship, although $\delta^{18}O$ values were scattered above and below the regression line, depending on the location with respect to the Andes flank. In the western part of the country the $\delta^{18}O$ values were below the general linear regression and showed more depleted values (< −12‰) than at comparable elevations in the east (> −12‰), as clearly evident in the contrasting values for La Maria and Albania (in the west) with Bogotá and El Hato (in the east). Two regression lines were obtained for the correlation between $\delta^{18}O$ weighted mean values and elevation for stations located on the Andes mountains (stations close to sea level were omitted as no considerable fractionation occurred). The first RL (slope of −0.23‰/100 m, $p = 0.01$) represented elevations from 1848 to 3150 m a.s.l. and included stations located to the east of the Central Colombian Andes. The second RL (slope of −0.10‰/100 m, $p = 0.07$) represented elevations from 2100 to 4413 m a.s.l., and encompassed stations located to the west of the Central Colombian Andes.

The equations for the RLs (Figure 8a–c) for stations P1, P2, and P3 were $\delta^2H = 8.02\ \delta^{18}O + 9.6$ ($R^2 = 0.98$), $\delta^2H = 8.94\ \delta^{18}O + 22.8$ ($R^2 = 0.97$), and $\delta^2H = 8.22\ \delta^{18}O + 15.1$ ($R^2 = 0.98$), respectively. These RLs were based solely on the periods of the sampling intervals in the years 2017 to 2018. For this reason, the effects of inter-seasonality, ENSO, or long-term meteorological parameters were not included, and the results are limited to the unique conditions of the sampled periods. The most depleted precipitation-weighted $\delta^{18}O$ values were found for samples having the highest accumulated precipitation at P1 and P3. The P1 and P2 values were similar, while the P3 values were more depleted, probably because of the increased effect of elevation. The overall RL equation for the UCRB was $\delta^2H = 8.2\ \delta^{18}O + 12.3$ ($R^2 = 0.98$) (Figure 9).

A comparison of RLs among locations in various geographical areas of Colombia, including the study site, is shown in Figure 10,

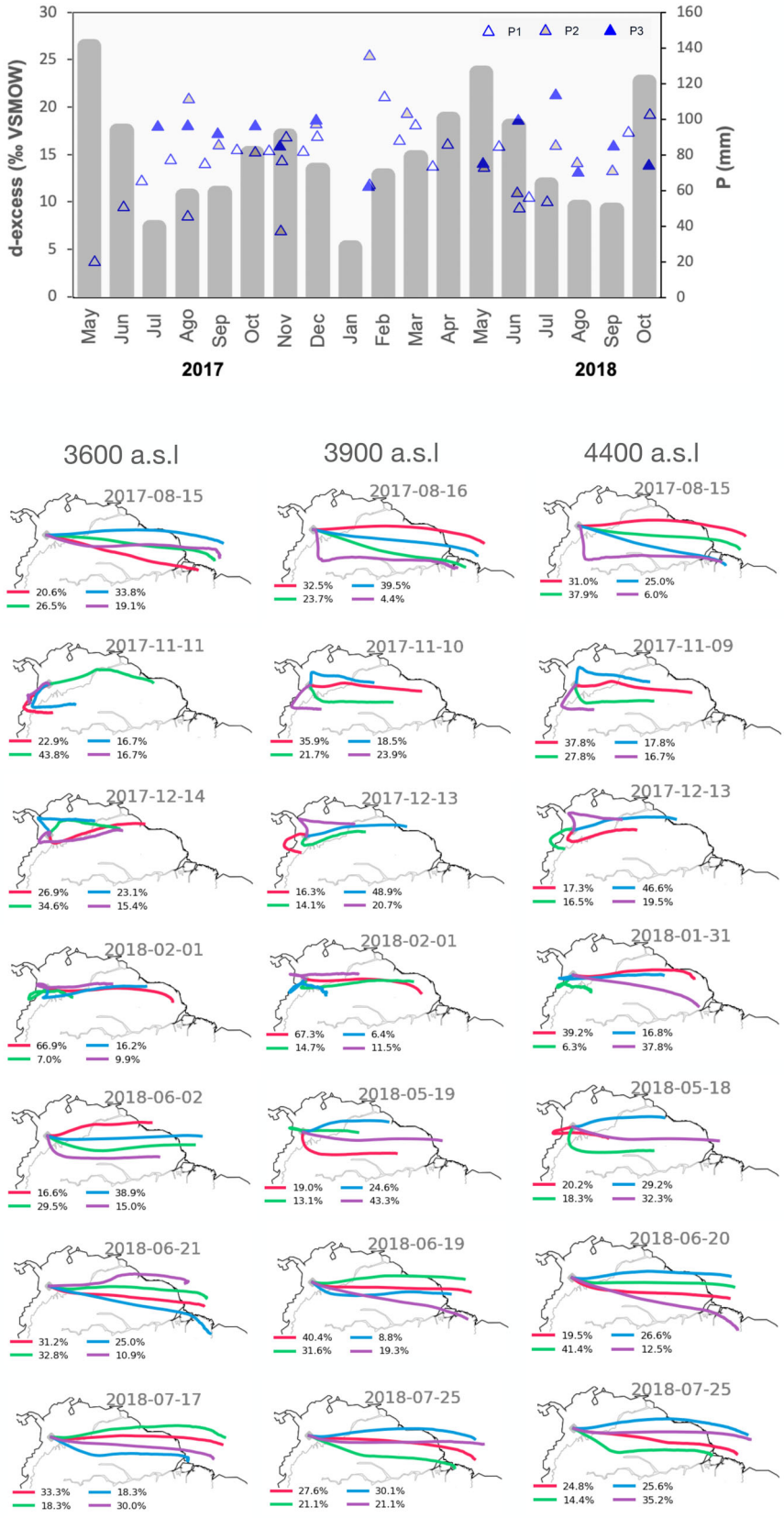

FIGURE 6 Upper: Variation in d-excess values for precipitation compared with monthly precipitation. Lower: back-trajectory analysis of air masses for the elevations of P1, P2, and P3 for precipitation sampling dates. Colours indicate the clusters and their respective percentage over the total trajectory ensemble. Grey lines indicate the limit of the Amazon basin and the Amazon River main branch.

and the results are summarized in Table 2. Long records were only available for Bogotá, while the other locations corresponded to short-term projects not exceeding 3 years. The data points represent the monthly average values for each station. The slopes for all lines are similar (ranging from 7.95 to 8.94) and close to the GMWL.

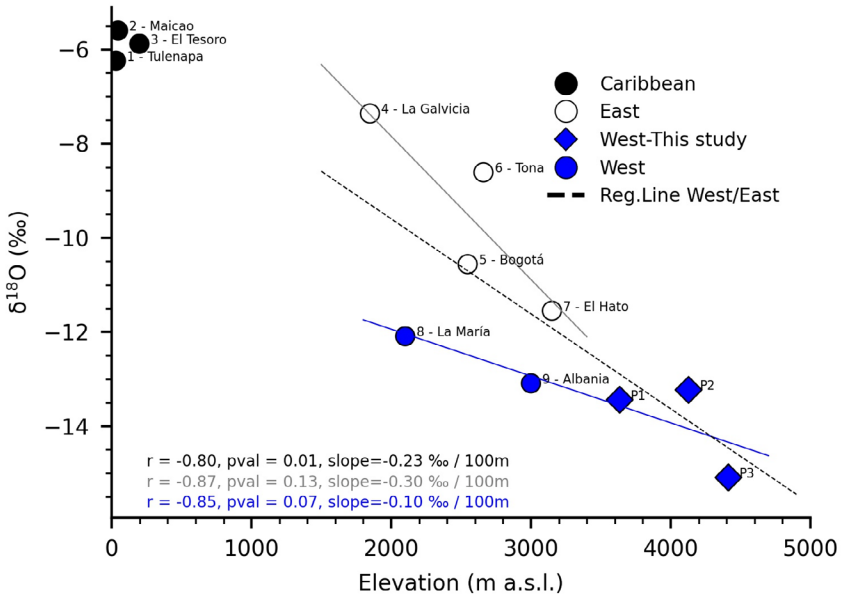

FIGURE 7 Relationship between $\delta^{18}O$ and elevation for GNIP stations in Colombia, grouped by location with respect to the Central Andes as a topographic reference separating areas having different wind mass sources, either from the Pacific Ocean (west) or from the Atlantic Ocean (east). The dashed regression line shows the precipitation-weighted $\delta^{18}O$ values for the east and west sides of the Central Andes.

4 | DISCUSSION

4.1 | Seasonality effect

The isotope composition of precipitation and stream water in the Andes Mountains is mostly driven by seasonal precipitation and atmospheric convective rain processes, and to a minor extent by temperature (Valdivielso et al., 2020). This is consistent with the findings of Vimeux et al. (2005), Saylor et al. (2009), and Balagizi et al. (2018), who reported that local temperature variations had a minor influence on the stable isotope values. A seasonal effect, as described by Clark and Fritz (1997) and Leibundgut et al. (2009) as the fluctuation of stable isotope composition in relation to temperature changes, cannot be interpreted for the UCRB as proposed by them. In the UCRB, temperature variations during the year are <4°C for the same elevation because of the low latitude, and therefore its effect could be evaluated only across elevational change. In the páramo the daily thermal amplitude in the dry season ranges from 22 to 30°C, while during the rainy season cloud cover results in the amplitude ranging from 12 to 18°C (Azócar & Rada, 2006). Thus, it is challenging to separate the effects of temperature and elevation when the precipitation patterns can also change across the ecosystems during the same day. The temperature effect could be better studied by measuring short-term stable isotope variations of rain or fog in páramo ecosystems.

The stream water stable isotope values were more depleted than those for precipitation. This pattern appears to be typical for rivers fed by higher elevation catchments (Yang et al., 2020), as has been reported for the high Andes mountains in Bolivia by Gonfiantini et al. (2001), and for the Peruvian Plateau by Bershaw et al. (2016). This pattern may be overlaid by specific high precipitation events occurring prior to the sampling day, or by snapshot sampling. Extremely depleted isotope values in the UCRB correlated with increasing stream discharge, typically during rainy months and specifically during high precipitation events. In this respect, Saylor et al. (2009) also found a clear effect of strong precipitation events on the stable isotope composition of precipitation and surface water in the Eastern Andes of Colombia. However, a mixture of heavy and light rain events in precipitation samples is likely to influence the isotope composition, suggesting an overlap with the amount effect found by Sturm et al. (2007) to dominant in South America during the rainy season. A clear example of the overlap between seasonality and amount effects was observed for stations S1and S2, where the most depleted $\delta^{18}O$ values during the entire study period occurred 1 week after the heaviest rainfall event (31.6 mm/day on 16 May 2017). Depleted isotope values were also recorded at stations S3 and S5 on 17 May 2017, demonstrating that the effect of heavy precipitation can be seen across the watershed.

The isotope values reported here do not reflect individual rain events in the UCRB. Even though higher levels of accumulated precipitation were associated with more depleted isotope values, this did not necessarily reflect an amount effect. The samplers collected for varying time periods, including in some cases 15 days and in others up to 95 days (Figure 3). Thus, despite the records suggesting an influence of greater precipitation amounts during the wet season on variation in the isotope composition, the irregular scale of sampling did not enable specific events be directly correlated with isotope composition data. According to Risi et al. (2008), the amount effect is best observed at intra-seasonal or longer timescales, as it is related to the residence time of water vapour in the atmosphere. This highlights the necessity for developing longer sampling campaigns at study sites, with at least monthly periodicity.

Variation in the $\delta^{2}H$ and $\delta^{18}O$ values for stream water at stations S1, S2, and S3, which are located downstream of the boundary between the Andean forest and the páramo (3400 m a.s.l.) was attenuated compared with upstream samples (Figure 4). This attenuation effect has been described by Gomez et al. (2015) in the Eastern Andes of Colombia. The low level of isotope variation, together with more enriched values, may be attributable to the Andean forest and the

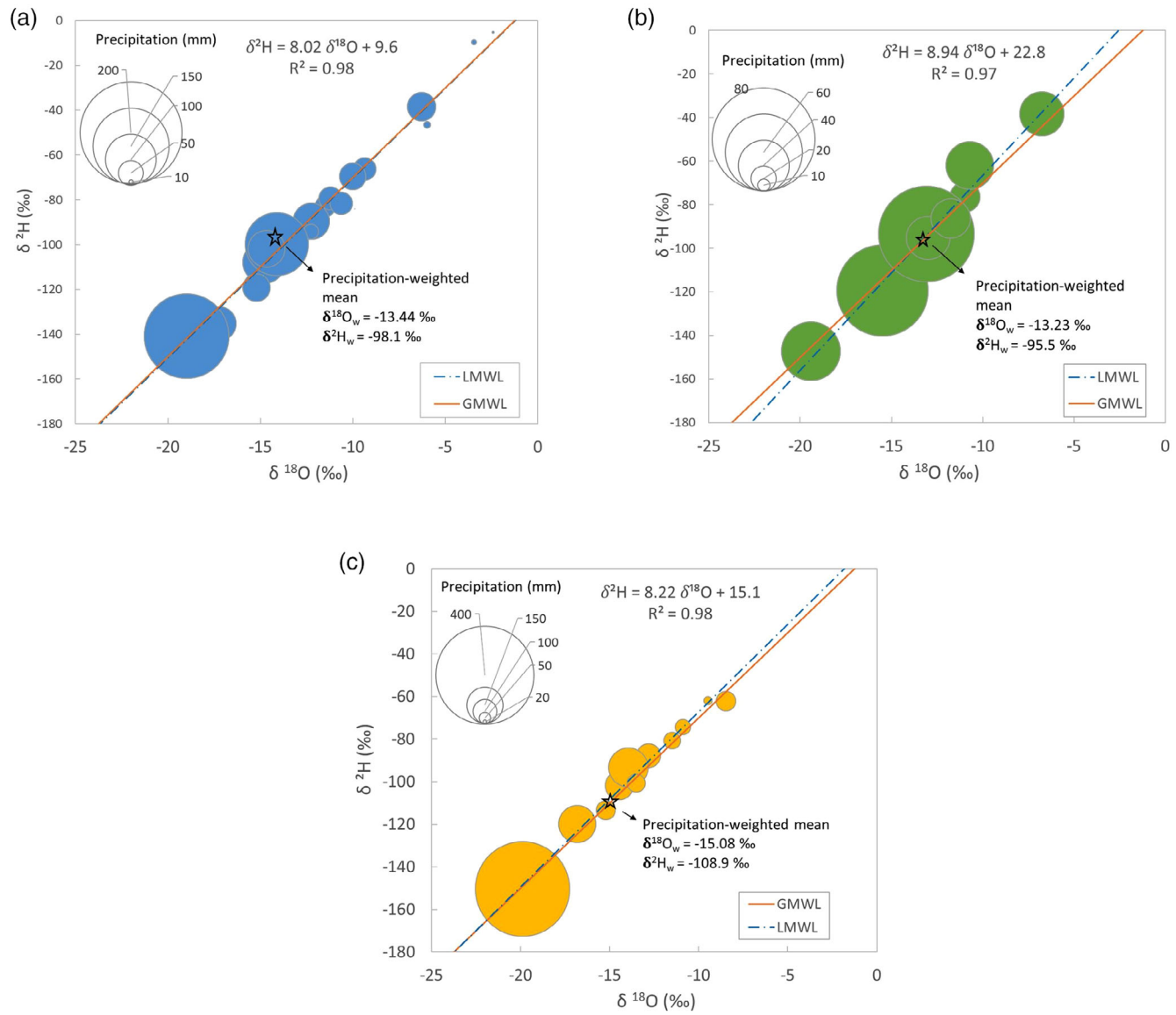

FIGURE 8 Plot of $\delta^{18}O$ versus $\delta^{2}H$ for precipitation samples collected at P1, P2, and P3, and the accumulated precipitation amount. The regression lines were drawn using the precipitation-weighted least square regression (PWLSR) method. The precipitation-weighted means for $\delta^{18}O$ and $\delta^{2}H$ were based on the entire sampling period. (a) Station P1 recorded the most depleted $\delta^{18}O$ value for the period having the highest level of accumulated precipitation (166 mm in the period 15 April 2018 to 2 June 2018), and the most enriched value for the lowest level of accumulated precipitation (5 and 6 mm in the periods 11 November 2017 to 15 November 2017 and 1 March 2018 to 16 March 2018, respectively) during the dry season. (b) Station P2 recorded the most depleted $\delta^{18}O$ value during rainy season (46 mm in the period 8 March 2018 to 19 May 2018). The most enriched value was detected during a wet period of dry months (35 mm during the period 1 February 2018 to 8 March 2018). (c) Station P3 recorded the most depleted $\delta^{18}O$ value for the period having the highest level of accumulated precipitation (386 mm in the period 31 January 2018 to 18 May 2018) and the most enriched value for the lowest level of accumulated precipitation (38 mm in the period 18 July 2018 to 15 July 2018) during the dry season.

cloud forest fringes acting as evaporative sources; this could have caused homogenization of the isotope signals. During the dry season, evaporation rates from lakes and vegetation are higher. Hence, we expected these sources to make a larger contribution to precipitation than air masses from outside the UCRB. This process could explain the isotope-enriched rain in the dry months of 2017 and 2018, which is also evident in the stream water isotope composition, an effect also observed in tropical regions of the Democratic Republic of Congo (Balagizi et al., 2018). Complementary hydrochemical samples from the hot spring (3600 m a.s.l.) and geological analyses in the UCRB have indicated an interrelationship between deep and shallow circulation waters. Therefore, we cannot exclude an influence from ^{18}O-enriched carbonate rocks, which occur widely in the geological basement of the Central Andes (Arango et al., 1970; Stewart et al., 1983).

While evaporation and hydrothermal activity might have dampened the isotope signals, other dampening factors have also been

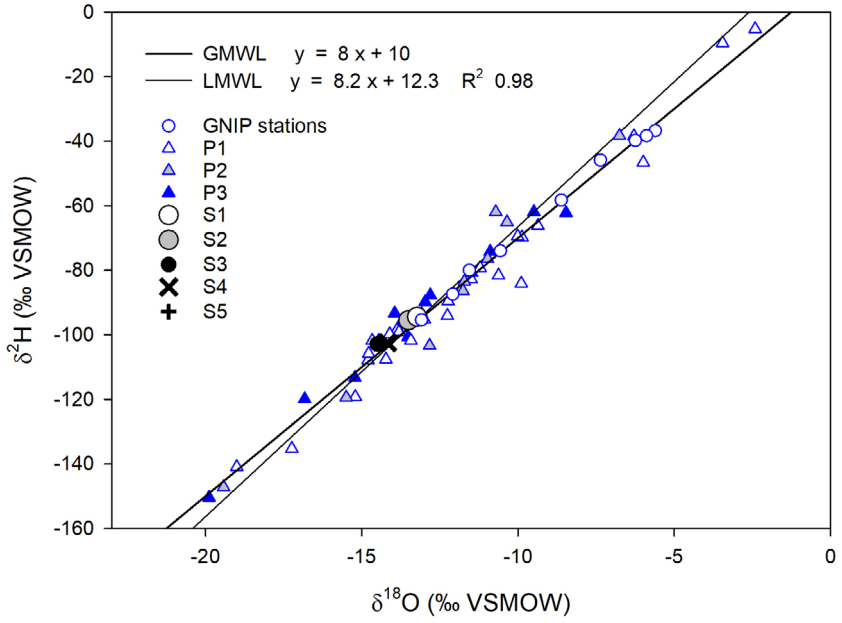

FIGURE 9 Relationship between $\delta^{18}O$ and $\delta^{2}H$ for all precipitation samples, showing regression lines (based on the PWLSR method) and mean values for the stream water stations. The lowest δ-values accounted for those samples from P1 and P3 having the highest levels of accumulated precipitation; for P2 this corresponded to an average accumulated precipitation sample located in the middle of the plot. The P1 and P2 values were similar, but the P3 values were more depleted, probably because of an increased altitude effect.

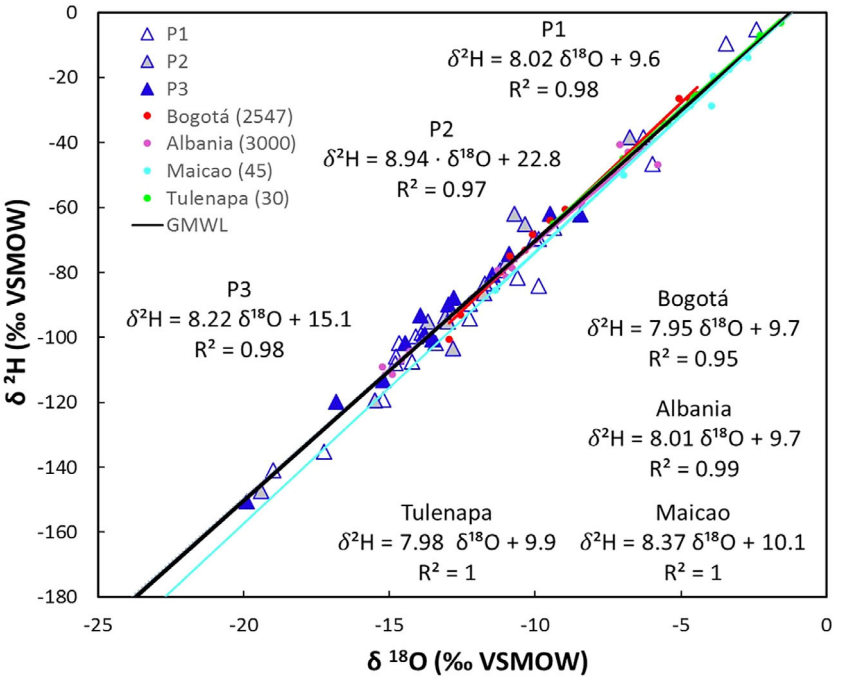

FIGURE 10 Compilation of regression lines (based on the PWLSR method) for precipitation stations in the study area and other regions of Colombia (Bogotá, Albania, Tulenapa, and Maicao), showing the monthly average values as filled circles. Data obtained from IAEA/WMO (2020).

proposed including: (i) the buffering effect of subsurface seepage from upper recharge areas, and discharges for peatland drainage networks, causing fractionation and so affecting the isotope composition (McDonnell et al., 1991; Sprenger et al., 2017); and (ii) mixing with surface water from upstream, previously documented in New Zealand mountain ranges having broad altitudinal ranges (Yang et al., 2020). To evaluate constraints on seasonal variations in the surface water isotope composition, further studies should include hydrogeological surveys of soils and the shallow subsurface interphase, and systematic mapping and sampling of hot springs and open bodies of water, which are common in the UCRB.

The $\delta^{2}H$ and $\delta^{18}O$ values for the three precipitation stations were generally variable and not homogeneously clustered, as a result of the influence of seasonality (variation in precipitation amounts) (Figure 8). The various slopes of the precipitation RLs and the stream water (SW) regression equation ($\delta^{2}H = 5.31\ \delta^{18}O - 25.8$, $R^2 = 0.79$) suggest that the surface water isotope composition was modified significantly by evaporation or mixing because of its location to the right of the GMWL, following the evaporation trend. The RL for the UCRB ($\delta^{2}H = 8.20\ \ \delta^{18}O + 12.3$, $R^2 = 0.98$) differs from that of the Colombian Meteoric Line proposed by Rodríguez (2004) ($\delta^{2}H = 8\ \delta^{18}O + 9.6$); this was not unexpected because in the present study

only precipitation from elevations above 3600 m a.s.l. during a different and relatively short time period were sampled. However, it is not clear if the evaporation or mixing occurred during rainfall, within the soil zone, or in the streams (Kendall & Coplen, 2001). Furthermore, while the occurrence of distillation processes can cause evaporation in the rainfall, the characteristics of precipitation and the origin of air masses could have an influence. In the UCRB the main wind direction is from the east during the rainy season and from the west during the dry season. The main wind patterns define the isotope composition observed in precipitation, because of the enhanced moisture recycling and mixing proportions that water vapour is subject to across differing orographic features in different months of the year.

The seasonal changes in the origin of air masses can be also interpreted according to the position of the ITCZ with respect to the study catchment area. During October and November, the ITCZ has a southward displacement, reaching its southernmost point in January (Poveda, 2004). During this time the ITCZ crosses the UCRB, and in January is south of our sampling locations, meaning that there is a stronger influence from the northeasterly trade winds into the northern part of the continent. This explains the northward shift of the clusters during the boreal winter described previously, which was related to the increased precipitation (Figure 6, upper panel) from September onwards in both years, indicating the approach and arrival of the ITCZ. From April to May the ITCZ moves northward (Poveda, 2004), and in July reached its northernmost location as the precipitation increased again from February to May in 2018. At that time the catchment area was located south of the ITCZ, and the northeasterly winds had lost their dominance; consequently, the clusters showed a more eastward direction.

Because the stable isotope composition changed seasonally, with more depleted values during the rainy season, we hypothesize that the origin of air mass plays an important role. This cannot be explained solely by the change in precipitation. As explained above, air mass origins change seasonally, and this defines the wet and dry months. Therefore, air masses from the Atlantic Ocean travelling across the Amazon rainforest for a large distance, in contrast to those coming from the Pacific Ocean, will result in a more depleted isotope composition because of more moisture recycling along the Atlantic-Amazon trajectory.

4.2 | Altitude effect

More depleted stable isotope values were found for the UCRB with increasing elevation, as described by the altitude effect (Dansgaard., 1954; Mook, 2000). However, the correlations of $\delta^{18}O$ and $\delta^{2}H$ values with elevation were non-linear for both precipitation and stream water. For example, it would be expected that the value for the precipitation-weighted mean for station P2 (−13.23‰) would have been between the values for P1 and P3 (−13.44 and −15.09‰) if there was a decrease in $\delta^{18}O$ with increased elevation, but the slopes of the correlations between elevation and $\delta^{18}O$ were not significantly different from zero. This effect was also described by Gonfiantini et al. (2001), who showed that the altitude effect deviates from linearity when elevation increases.

The non-linear altitude effect for precipitation samples occurred between 3635 and 4128 m a.s.l. (from P1 to P2), and can be attributed to more depleted PW mean $\delta^{18}O$ values for P1 compared to P2, resulting in a very local positive elevation gradient. Studies in the Ailao Mountains (Jiao et al., 2019) and the Rocky Mountains (Moran et al., 2007) have interpreted these heterogeneities or inverse altitude effects to the influence of the local water cycle and mixed moisture sources. For example, an increase in the contribution of local moisture could mask an elevation effect (Jiao et al., 2019), or the contribution of vapour masses to both lee and windward slopes could cause a depletion of $\delta^{18}O$ with distance as precipitation occurs (Moran et al., 2007). In the UCRB the very depleted $\delta^{18}O$ values found for P1 caused the positive altitude effect with respect to P2; in this case the samples were collected during the first rainy season (MAM), when predominant air masses included a mixture of east and west sources (Figure 6). We argue that such depleted values can be explained by an ongoing Rayleigh distillation of the moisture coming from the east, and precipitation occurring after the air masses cross over the top of the Andes. Our study did not investigate inter-seasonal effects, and therefore we were unable to quantitatively assess this hypothesis; however, we concluded that there was a significant influence of seasonality and the type of slope on the altitude effect. To cope with such uncertainty, more comprehensive (covering more elevation stations) and long-term (at least 5 years) stable isotope composition sampling should be conducted.

In the stream water samples the influence of seasonality on variation in the $\delta^{18}O$ values was clearly evident. At higher elevations, closer to the glacier (P3), precipitation had a greater effect on the stream water at S4 and S5 than downstream at S2, as the catchment area was smaller upwards and most of the runoff was the result of precipitation. Therefore, higher elevation samples recorded the signal of seasonally-depleted precipitation events. For instance, stream water in the upper basin showed isotope values similar to rain (S4 and S5 vs. P3) relative to lower elevations (S2 vs. P1). At lower elevations (<4100 m a.sl.), buffering effects probably caused by upstream water mixing and contributions from hot springs could explain the low variability of the isotope values. Furthermore, although the Conejeras glacier represents a very small percentage of the drainage area, the fact that S5 is at the outlet of the glacier suggests that data from this station may provide hints regarding the isotope variability caused by ice and snow melting at both the daily and seasonal time scales (Morán-Tejeda et al., 2018). Snowfall is a common phenomenon in the catchment at elevations >4800 m a.s.l., but generally lasts only for a very short time (hours or several days) outside the glaciated area. Even if the presence of snow is rare for most parts of the catchment, a more careful analyses of the isotope signal of snowfall and snowpack, and more intense sampling of the water melting from the glacier would be helpful in understanding the hydrology of the watershed.

The altitude effect on precipitation found in this study is slightly lower than the altitude effect proposed for all of Colombia (−0.25‰ $\delta^{18}O$/100 m; Rodríguez, 2004), but is similar to that reported for

other tropical regions (−0.20‰ $\delta^{18}O$/100 m: Cortes et al., 1997; and −0.22‰ $\delta^{18}O$/100 m: Windhorst et al., 2013); this is because our data encompassed extremely high elevations (>3600 m a.s.l.). The gradient reported in our study is consistent with those reported for the southern slope of the Himalaya (−0.17‰/100 m) (Acharya et al., 2020) and the Lebanon and Anti-Lebanon mountains (−0.15‰ and −0.14‰/100 m, respectively) (Koeniger et al., 2016, 2017), and is generally in the ranges proposed by Windhorst et al. (2013) (−0.1 to −0.6‰ $\delta^{18}O$/100 m) and Siegenthaler and Oeschger (1980) (−0.4 to −0.16‰ of $\delta^{18}O$/100 m), based on data from Europe for elevations of 500–2000 m a.s.l. The altitude effect of stream water (−0.11‰/100 m) is less that that reported for Ecuador (−0.17‰/100 m; García et al., 1997), and for multiple sites on the Eastern Andes of Colombia (−0.18‰/100 m; Saylor et al., 2009), which indicates that altitude effects may differ with varying elevation. Despite the contrasting latitude and elevation conditions for which other gradients have been calculated, the values in the UCRB are consistent and comparable to other locations.

Based on several GNIP stations across Colombia, two spatially-distinct gradients can be distinguished, separated by the dividing line of the Central Andes. From our results, it is evident that despite the elevation of the Bogotá station (2600 m a.s.l.; Eastern Andes), the values of $\delta^{18}O$ for P1, P2, and P3 would not match those for the Eastern Andes if the altitude gradient found for the UCRB were used to calculate it. Similarly, the Eastern Andes showed more enriched $\delta^{18}O$ values than the Western Andes, probably because of its proximity to evaporation sources including the Caribbean Sea and the Amazon forest. A similar contrast between the eastern and the western slopes of the Central Andes was also found 40 km south of the UCRB by Piña et al. (2018). In that study the different air mass sources affecting the eastern and the western sides of the Andes were thought to explain the observed difference in altitude effects. Studies in other mountain ranges including in southwest France (Zhang et al., 2020) and China (Jiao et al., 2020) have reported the marked influence of moisture sources on the isotope composition of precipitation. Wind direction and atmospheric circulation studies (Hoyos et al., 2018; IDEAM & UPME, 2017) have indicated that the UCRB is a convergent region for moisture from several directions throughout the year. The proportions and influence of these moisture sources explain the contrasting altitude gradients between the two domains separated by the Colombian Central Andes: one towards the east and the other towards the west, as suggested in this study.

4.3 | d-excess

The most positive precipitation d-excess values occurred during dry months, and the most negative values occurred during the rainy months. The variation in d-excess suggests that high values are mainly a consequence of recycled moisture and relative humidity changes, as reported for the Mediterranean Sea region (Koeniger et al., 2016, 2017). The occurrence of more positive d-excess values in dry periods associated with moisture recycling enhanced by local evapotranspiration has been also reported for Costa Rica by Sánchez-Murillo et al. (2017). For the area involved in the present study, this phenomenon can be explained by the sources of rain during the wet and dry seasons. During the first DJF dry season, the main wind directions are from the Caribbean Sea and the Pacific Ocean, passing through the CTMF (Figure 1). However, these air masses do not contribute a considerable amount of humidity from the original evaporative source, which is reflected in the relative low precipitation recorded during this period. The precipitation that occurred in the páramo during the dry seasons had the most positive d-excess values as a result of air masses transported from a continental evaporation source such as the Amazon forest (Esquivel-Hernández et al., 2019). Hence, rainfall events during the less humid seasons may have been produced after repeated local recycling episodes, with inputs from high retention reservoirs including lakes and soils, which occur throughout these high mountain ecosystems (Martinelli et al., 1996; Ramón-Reinozo et al., 2019).

Atmospheric moisture from the Tropical North Atlantic (TNA) crossing the Amazon basin makes up the largest proportion of precipitable water in northern South America during the DJF dry season (Agudelo et al., 2019; Ruiz-Vásquez et al., 2020). Although there are few studies comparing the isotope composition in the Colombian Central Andes with that of the Amazon basin, our back-trajectory simulations are consistent with recent findings by Escobar et al. (2022), and wind direction models developed by IDEAM and UPME (2017), Arias et al. (2015), and Sakamoto et al. (2011). The UCRB receives a considerable amount of moisture that has previously crossed the Amazon forest and the Eastern Andes from the TNA. This trajectory contributes to increase of precipitation d-excess because of successive evaporation cycles during transit from the TNA, and from local cycling.

Our back-trajectory results indicate that during the rainy season the main atmospheric moisture sources in the UCRB are from the Tropical South Atlantic (TSA) and the northern Amazon (NAMZ) (Agudelo et al., 2019; IDEAM & UPME, 2017). Several episodes of fractionation and recycling associated with the Amazon forest and the ascent of air through the Andes occurred in the trade winds (Vallet-Coulomb et al., 2008). Consequently, the d-excess values are mainly affected by the amount of atmospheric moisture coming from the Amazon basin, and the intensity of the moisture recycling in this precipitable water. The influence of local ecosystems and land cover may play additional important roles, as they directly affect transpiration and atmospheric circulation by enhancing evapotranspiration (Escobar et al., 2022; Hoyos et al., 2018).

The influence on d-excess values of local processes including soil evaporation (Jouzel et al., 2013), mixing sources, and recycled air moisture (Froehlich et al., 2002) should be considered in future analyses. In practice, these can be investigated through longer term isotope monitoring programs that enhance understanding of the influence of open water and land cover on evaporation processes, as proposed by Henderson-Sellers and McGuffie (2006). An approach considering event-based sampling could investigate temporal and spatial convective impacts on the isotope composition of precipitation

(Vimeux et al., 2011). Although Gat et al. (2001) argues that precipitation at the crest of the Andes slopes results from the Atlantic Ocean, and at lower elevations from the Pacific Ocean, the processes are likely to be more complex, particularly in the Colombian Andes. This study demonstrates a high level of complexity among factors influencing the isotope composition of rain and stream water in northern South America.

5 | CONCLUSIONS

This study provides a comprehensive analysis of the spatiotemporal variation of stable isotopes in the UCRB for the period 2017 to 2018. The isotope values were more depleted during the rainy season. We showed that a seasonal effect was determined by wet-dry cycles, and overlaid by the amount effect. Temperature patterns did not determine variations in the stable isotope composition. A reduction in variation in the composition of stable isotopes in stream water was observed downstream from 3400 m a.s.l., below the boundary between the páramo and the Andean forest, suggesting that ecosystem type and land cover may be driving factors affecting the spatiotemporal distribution.

Two contrasting altitude gradients separated by the dividing line of the Central Andes were observed. The altitude effect for precipitation (−0.18‰/100 m) was non-linear, and comparable to that found in other studies in the Tropical Andes. Most positive d-excess values occurred during dry months, and were affected by the ITCZ position and the mixed air masses travelling from the Amazon forest across the Andes Mountains. These values were apparently enhanced by moisture recycling generated in the páramo, cloud forest, and Andean forest ecosystems, although more data are necessary to test this possibility. The Central Andes are under the influence of two climatic regimes (Atlantic and Pacific), which are the main air mass sources. The variety of source areas, and geological, topographic, and ecosystem features, provides a new focus for hydrological research in the northern Andes.

Our study fills information gaps in a region that has been poorly studied, and builds on several studies suggesting the influence of the Chocó Stream and the Tropical North Pacific basin as evaporative sources for precipitation in the Central Colombian Andes. The absence of stable isotope studies in the Chocó region has hindered analysis of the magnitude and seasonality of stable isotope variation. We argue that the hydrology of Andean ecosystems must be understood as part of a wider and more complex system. The páramos and glaciers provide clear evidence that precipitation originates not only from the evapotranspiration of water in high mountain areas, but also from ecosystems at lower elevations, including cloud forest, the Andean forest, and the Amazon rainforest. As a consequence, the ongoing delimitation of water supply basins and definition of boundaries between ecosystems in the high-mountains of Colombia, and long-term goals in territorial planning for the country, should consider boundaries beyond those strictly based on ground-based characteristics.

ACKNOWLEDGEMENTS

This work was developed with the technical advice of the Instituto de Hidrología, Meteorología y Estudios Ambientales (IDEAM) in Colombia and partially sponsored by the German Academic Exchange Service (DAAD) of Germany within the framework of the development-related postgraduate course (EPOS) program and the project MARGISNOW (PID2021-124220OB-100) (Spanish Ministry of Science and Innovation). The stable isotopes analyses were conducted by the Stable Isotopes Laboratory of the Colombian Geological Survey (SGC). The Max Planck Institute for Biogeochemistry partially supported ATE and SB and the Technical University of Braunschweig partially supported ATE. We would like to thank Nils Michelsen and Christoph Schüth for their valuable contributions, Katharina Dulias for the proofreading of a preliminar version of this manuscript, Andrés Porras for sample analyses, Francisco Rojas for facilitating meteorological data acquisition, and finally, Andrés Aguilar and Carlos Vergara for their advice on data processing. Open Access funding enabled and organized by Projekt DEAL through the Max Planck Institute for Biogeochemistry.

CONFLICT OF INTEREST STATEMENT

The authors declare no conflict of interest.

DATA AVAILABILITY STATEMENT

Results of the stable isotope analyses can be found and downloaded from https://zenodo.org/record/7716975#.ZAtPcuzMKCi (Tangarife-Escobar et al., 2023).

ORCID

Andrés Tangarife-Escobar https://orcid.org/0000-0001-5185-0011
Paul Koeniger https://orcid.org/0000-0002-1197-6274
Juan Ignacio López-Moreno https://orcid.org/0000-0002-0900-3473
Santiago Botía https://orcid.org/0000-0002-5447-3968

REFERENCES

Acharya, S., Yang, X., Yao, T., & Shrestha, D. (2020). Stable isotopes of precipitation in Nepal Himalaya highlight the topographic influence on moisture transport. *Quaternary International*, *565*, 22–30. https://doi.org/10.1016/j.quaint.2020.09.052

Agudelo, J., Arias, P. A., Vieira, S. C., & Martínez, J. A. (2019). Influence of longer dry seasons in the southern Amazon on patterns of water vapor transport over northern South America and the Caribbean. *Climate Dynamics*, *52*(5–6), 2647–2665. https://doi.org/10.1007/s00382-018-4285-1

Ampuero, A., Stríkis, N. M., Apaéstegui, J., Vuille, M., Novello, V. F., Espinoza, J. C., Cruz, F. W., Vonhof, H., Mayta, V. C., Martins, V. T. S., Cordeiro, R. C., Azevedo, V., & Sifeddine, A. (2020). The forest effects on the isotopic composition of rainfall in the northwestern Amazon Basin. *Journal of Geophysical Research-Atmospheres*, *125*(4). https://doi.org/10.1029/2019JD031445

Arango, E. E., Buitrago, A. J., Cataldi, R., Ferrara, G. C., Panichi, C., & Villegas, V. J. (1970). Preliminary study on the Ruiz geothermal project (Colombia). *Geothermics*, *2*(Part 1), 43–56. https://doi.org/10.1016/0375-6505(70)90005-2

Arias, P. A., Martínez, J. A., & Vieira, S. C. (2015). Moisture sources to the 2010–2012 anomalous wet season in northern South America. *Climate Dynamics*, *45*(9–10), 2861–2884. https://doi.org/10.1007/s00382-015-2511-7

Azócar, A., & Rada, F. (2006). *Ecofisiología de plantas de páramo* (p. 175). Universidad de los Andes.

Balagizi, C. M., Kasereka, M. M., Cuoco, E., & Liotta, M. (2018). Influence of moisture source dynamics and weather patterns on stable isotopes ratios of precipitation in central-eastern Africa. *Science of the Total Environment*, *628–629*, 1058–1078. https://doi.org/10.1016/j.scitotenv.2018.01.284

Benetti, M., Reverdin, G., Pierre, C., Merlivat, L., Risi, C., Steen-larsen, H. C., & Vimeux, F. (2014). Deuterium excess in marine water vapor: Dependency on relative humidity and surface wind speed during evaporation. *Journal of Geophysical Research-Atmospheres*, *119*, 584–593. https://doi.org/10.1002/2013JD020535

Bershaw, J., Hansen, D. D., & Schauer, A. J. (2020). Deuterium excess and 17O-excess variability in meteoric water across the Pacific northwest, USA. *Tellus Series B: Chemical and Physical Meteorology*, *72*(1), 1–17.

Bershaw, J., Saylor, J. E., Garzione, C. N., Leier, A., & Sundell, K. E. (2016). Stable isotope variations ($\delta^{18}O$ and δD) in modern waters across the Andean plateau. *Geochimica et Cosmochimica Acta*, *194*, 310–324. https://doi.org/10.1016/j.gca.2016.08.011

Betancur, T., & Palacio, P. (2007). Identificación de fuente y zonas de recarga a un sistema acuífero a partir de isótopos estables del agua. *Investigación*, *10*, 167–182.

Bohórquez, O., Monsalve, M., Velandia, F., Gil, F., & Mora, H. (2005). Tectonic setting of the northernmost Volcanic Belt of the central cordillera, Colombia. *Boletin de Geologia*, *27*(1), 55–79.

Buytaert, W. (2004). The properties of the soils of the south Ecuadorian páramo and the impact of land use changes on their hydrology [Unpublished Ph.D. thesis], Katholieke Universiteit Leuven.

Buytaert, W., Célleri, R., De Bièvre, B., Cisneros, F., Wyseure, G., Deckers, J., & Hofstede, R. (2006). Human impact on the hydrology of the Andean páramos. *Earth-Science Reviews*, *79*(1–2), 53–72. https://doi.org/10.1016/j.earscirev.2006.06.002

Buytaert, W., Sevink, J., Leeuw, B. D., & Deckers, J. (2005). Clay mineralogy of the soils in the south Ecuadorian páramo region. *Geoderma*, *127*, 114–129.

Campillo, A., Taupin, J. D., Betancur, T., Patris, N., Vergnaud, V., Paredes, V., & Villegas, P. (2021). A multi-tracer approach for understanding the functioning of heterogeneous phreatic coastal aquifers in humid tropical zones. *Hydrological Sciences Journal*, *66*(4), 600–621.

Carslaw, D. C., & Ropkins, K. (2012). Openair—An R package for air quality data analysis. *Environmental Modelling and Software*, *27–28*, 52–61. https://doi.org/10.1016/j.envsoft.2011.09.008

Castrillon, F., Quiroz, O., Bermoudes, O., & Aravena, R. (2003). Evaluation of the origin and residence time of the groundwater in a regional aquifer system, Rio de Bogotá basin, Colombia. In *International symposium on isotope hydrology and integrated water resources management* (pp. 229–230). IAEA.

Ceballos, J. L., Euscátegui, C., Ramírez, J., Cañon, M., Huggel, C., Haeberli, W., & Machguth, H. (2006). Fast shrinkage of tropical glaciers in Colombia. *Annals of Glaciology*, *43*, 194–201. https://doi.org/10.3189/172756406781812429

Clark, I., & Fritz, P. (1997). *Environmental isotopes in hydrogeology*. CRC press.

Cortes, A., Durazo, J., & Farvolden, R. N. (1997). Studies of isotopic hydrology of the basin of Mexico and vicinity: Annotated bibliography and interpretation. *Journal of Hydrology*, *198*, 346–376.

Craig, H. (1961). Isotope variations in meteoric waters. *Science*, *133*, 1702–1703.

Crawford, J., Hughes, C. E., & Lykoudis, S. (2014). Alternative least squares methods for determining the meteoric water line, demonstrated using GNIP data. *Journal of Hydrology*, *519*, 2331–2340. https://doi.org/10.1016/j.jhydrol.2014.10.033

Dansgaard, W. (1964). Stable isotopes in precipitation. *Tellus*, *16*(4).

Dansgaard, V. (1954). Oxygen-18 abundance in fresh water. *Geochimica et Comochimica Acta*, *6*, 241–260.

Escobar, M., Hoyos, I., Nieto, R., & Villegas, J. C. (2022). The importance of continental evaporation for precipitation in Colombia: A baseline combining observations from stable isotopes and modelling moisture trajectories. *Hydrological Processes*, *36*(6), e14595.

Esquivel-Hernández, G., Mosquera, G. M., Sánchez-Murillo, R., Quesada-Román, A., Birkel, C., Crespo, P., Célleri, R., Windhorst, D., Breuer, L., & Voll, J. (2019). Moisture transport and seasonal variations in the stable isotopic composition of rainfall in central American and Andean Páramo during El Niño conditions (2015–2016). *Hydrological Processes*, *33*(13), 1802–1817. https://doi.org/10.1002/hyp.13438

Fiorella, R. P., Poulsen, C. J., Zolá, R. S. P., Barnes, J. B., Tabor, C. R., & Ehlers, T. A. (2015). Spatiotemporal variability of modern precipitation $\delta^{18}O$ in the Central Andes and implications for paleoclimate and paleoaltimetry estimates. *Journal of Geophysical Research: Atmospheres*, *120*, 4630–4656. https://doi.org/10.1002/2014JD022893

Froehlich, K., Gibson, J. J., & Aggarwal, P. K. (2002). *Deuterium excess in precipitation and its climatological significance* (No. IAEA-CSP-13/P). International Atomic Energy Agency.

Froehlich, K., Kralik, M., Papesch, W., Rank, D., Scheifinger, H., & Stichler, W. (2008). Deuterium excess in precipitation of alpine regions–moisture recycling. *Isotopes in Environmental and Health Studies*, *44*(1), 61–70.

Gat, J. R., Mook, W. G., & Meijer, H. A. (2001). Environmental isotopes in the hydrological cycle. *Principles and Applications UNESCO/IAEA Series*, *2*, 63–67.

García, M., Villalba, F., Araguás-Araguás, L., & Rozanski, K. (1997). The role of atmospheric circulation patterns in controlling the regional distribution of stable isotope contents in precipitation: Preliminary results from two transects in the Ecuadorian Andes. In *Isotope Techniques in The Study of Environmental Change: Proceedings of a Symposium* (pp. 127–141). International Atomic Energy Agency (IAEA).

Gomez, S., Taupin, J. D., & Rueda, A. (2015). Estudio hidrodinámico, geoquímico e isotópico de las formaciones acuíferas de la región de Bucaramanga (Colombia). *Revista Peruana Geo-Atmosferica RPGA*, *4*, 44–61.

Gonfiantini, R. (1998). On the isotopic composition of precipitation. In F. Causse & C. Gasse (Eds.), *Hydrology and isotope geochemistry*. International Atomic Energy Agency (IAEA).

Gonfiantini, R., Roche, M., Olivry, J., Fontes, J., & Zuppi, G. (2001). The altitude effect on the isotopic composition of tropical rains. *Chemical Geology*, *181*, 147–167.

Harden, C. P., Hartsig, J., Farley, K. A., Lee, J., & Bremer, L. L. (2013). Effects of land-use change on water in Andean Páramo grassland soils. *Annals of the Association of American Geographers*, *103*(2), 375–384. https://doi.org/10.1080/00045608.2013.754655

Hastenrath, S. (2002). The intertropical convergence zone of the eastern Pacific revisited. *International Journal F: Climatology*, *22*(3), 347–356. https://doi.org/10.1002/joc.739

Henderson-Sellers, A., & McGuffie, K. (2006). Shift in stable water isotopes in precipitation in the Andean Amazon: Implications of deforestation or greenhouse impacts?. *Radioactivity in the Environment*, *8*, 39–49. https://doi.org/10.1016/S1569-4860(05)08003-4

Hofstede, R. (2003). Los Páramos del mundo. In P. Segarra & P. M. Vásconez (Eds.), *Proyecto Atlas Mundial de los Páramos* (p. 297). Global Peatland Initiative/NC-IUCN/EcoCiencia.

Hofstede, R. G. M. (1995). Effects of livestock farming and recommendations for management and conservation of páramo grasslands (Colombia). *Land Degradation and Rehabilitation*, *6*, 133–147.

Hoyos, I., Dominguez, F., Cañón-Barriga, J., Martínez, J. A., Nieto, R., Gimeno, L., & Dirmeyer, P. A. (2018). Moisture origin and transport

processes in Colombia, northern South America. *Climate Dynamics*, *50*(3–4), 971–990. https://doi.org/10.1007/s00382-017-3653-6

Hughes, C. E., & Crawford, J. (2012). A new precipitation weighted method for determining the meteoric water line for hydrological applications demonstrated using Australian and global GNIP data. *Journal of Hydrology*, *464–465*, 344–351. https://doi.org/10.1016/j.jhydrol.2012.07.029

Hurley, J. V., Galewsky, J., Worden, J., & Noone, D. (2012). A test of the advection-condensation model for subtropical water vapor using stable isotopologue observations from Mauna Loa observatory, Hawaii. *Journal of Geophysical Research*, *117*, D19118. https://doi.org/10.1029/2012JD018029

Hurley, J. V., Vuille, M., Hardy, D. R., Burns, S. J., & Thompson, L. G. (2015). Cold air incursions, O-18 variability, and monsoon dynamics associated with snow days at Quelccaya ice cap, Peru. *Journal of Geophysical Research-Atmospheres*, *120*(15), 7467–7487. https://doi.org/10.1002/2015JD023323

IAEA/WMO. (2020). *Global network of isotopes in precipitation*. The GNIP Database. https://nucleus.iaea.org/wiser.

IDEAM. (2011). *Mapas de precipitacion en Colombia*. http://www.ideam.gov.co/documents/21021/21141/precip+media+%5BModo+de+compatibilidad%5D.pdf/e0ae03be-8e3a-44f8-b5a2-2148a5aeff4d.

IDEAM & UPME. (2017). *Atlas de viento de Colombia*. IDEAM & UPME.

IPBES. (2019). In E. S. Brondizio, J. Settele, S. Díaz, & H. T. Ngo (Eds.), *Global assessment report on biodiversity and ecosystem services of the intergovernmental science-policy platform on biodiversity and ecosystem services* (p. 1148). IPBES secretariat. https://doi.org/10.5281/zenodo.3831673

IPCC. (2022). In H.-O. Pörtner, D. C. Roberts, M. Tignor, E. S. Poloczanska, K. Mintenbeck, A. Alegría, M. Craig, S. Langsdorf, S. Löschke, V. Möller, A. Okem, & B. Rama (Eds.), *Climate change 2022: Impacts, adaptation, and vulnerability. Contribution of working group II to the sixth assessment report of the intergovernmental panel on climate change*. Cambridge University Press.

Jiao, Y., Liu, C., Gao, X., Xu, Q., Ding, Y., & Liu, Z. (2019). Impacts of moisture sources on the isotopic inverse altitude effect and amount of precipitation in the Hani Rice terraces region of the Ailao Mountains. *Science of the Total Environment*, *687*, 470–478. https://doi.org/10.1016/j.scitotenv.2019.05.426

Jiao, Y., Liu, C., Liu, Z., Ding, Y., & Xu, Q. (2020). Impacts of moisture sources on the temporal and spatial heterogeneity of monsoon precipitation isotopic altitude effects. *Journal of Hydrology*, *583*, 124576. https://doi.org/10.1016/j.jhydrol.2020.124576

Jouzel, J., Delaygue, G., Landais, A., Masson-Delmotte, V., Risi, C., & Vimeux, F. (2013). Water isotopes as tools to document oceanic sources of precipitation. *Water Resources Research*, *49*(11), 7469–7486. https://doi.org/10.1002/2013WR013508

Jouzel, J., & Merlivat, L. (1984). Deuterium and oxygen 18 in precipitation: Modeling of the isotopic effects during snow formation. *Journal of Geophysical Research-Atmospheres*, *89*(D7), 11749–11757.

Kendall, C., & Coplen, T. B. (2001). Distribution of oxygen-18 and deuteriun in river waters across the United States. *Hydrological Processes*, *15*(7), 1363–1393. https://doi.org/10.1002/hyp.217

Koeniger, P., Margane, A., Abu-Rizk, J., & Himmelsbach, T. (2017). Stable isotope studies on altitude effect and karst groundwater catchment delineation of the Jeita spring in Lebanon. *Hydrological Processes*, *31*, 3708–3718. https://doi.org/10.1002/hyp.11291

Koeniger, P., Toll, M., & Himmelsbach, T. (2016). Stable isotopes of precipitation and spring waters reveal an altitude effect in the Anti-Lebanon Mountains, Syria. *Hydrological Processes*, *30*(16), 2851–2860. https://doi.org/10.1002/hyp.10822

Leibundgut, C., Maloszewski, P., & Külls, C. (2009). *Tracers in hydrology*. Wiley-Backwell.

Lin, J. C., Gerbig, C., Wofsy, S. C., Andrews, A. E., Daube, B., Davis, K., & Grainger, C. A. (2003). A near-field tool for simulating the upstream influence of atmospheric observations: The stochastic time- inverted Lagrangian transport (STILT) model. *Journal of Geophysical Research*, *108*, ACH 2-1–ACH 2-17. https://doi.org/10.1029/2002JD003161

Luteyn, J. L. (1992). Páramos: Why study them? In H. Balslev & J. L. Luteyn (Eds.), *Páramo: An Andean ecosystem under human influence* (pp. 1–14). Academic Press.

Mariño-Martinez, J., Veloza-Franco, J., & Martínez-Sánchez, A. (2018). Analysis of precipitation and recharge of aquifers in Tota and Ibagué (Colombia) from stable isotopes (^{18}O and ^{2}H). *Revista Facultad de Ingeniería*, *27*(47), 61–71.

Martinelli, L. A., Victoria, R. L., Sternberg, L. S. L., Ribeiro, A., & Moreira, M. Z. (1996). Using stable isotopes to determine sources of evaporated water to the atmosphere in the Amazon basin. *Journal of Hydrology*, *183*(3–4), 191–204. https://doi.org/10.1016/0022-1694(95)02974-5

McDonnell, J. J., Stewart, M. K., & Owens, I. F. (1991). Effect of catchment-scale subsurface mixing on stream isotopic response. *Water Resources Research*, *27*(12), 3065–3073. https://doi.org/10.1029/91WR02025

Medina, G., Paez, G., Vargas, M., & Taupin, G. (2009). Estudio Hidrogeológico con Enfasis en Hidrogeoquímica de los Acuíferos en la Zona Sur del Departamento del Valle del Cauca (Colombia). *Estudios de Hidrología Isotópica En América Latina*, *2006*, 47–65.

Mook, W. G. (2000). *Environmental isotopes in the hydrological cycle: principles and applications*. IAEA-UNESCO.

Mölg, N., Ceballos, J. L., Huggel, C., Micheletti, N., Rabatel, A., & Zemp, M. (2017). Ten years of monthly mass balance of Conejeras glacier, Colombia, and their evaluation using different interpolation methods. *Geografiska Annaler. Series A: Physical Geography*, *99*(2), 155–176. https://doi.org/10.1080/04353676.2017.1297678

Moran, T. A., Marshall, S. J., Evans, E. C., & Sinclair, K. E. (2007). Altitudinal gradients of stable isotopes in lee-slope precipitation in the Canadian Rocky Mountains. *Arctic, Antarctic, and Alpine Research*, *39*(3), 455–467. https://doi.org/10.1657/1523-0430(06-022)[MORAN]2.0.CO;2

Morán-Tejeda, E., Luis Ceballos, J., Peña, K., Lorenzo-Lacruz, J., & López-Moreno, I. J. (2018). Recent evolution and associated hydrological dynamics of a vanishing tropical Andean glacier: Glaciar de Conejeras, Colombia. *Hydrology and Earth System Sciences*, *22*(10), 5445–5461. https://doi.org/10.5194/hess-22-5445-2018

Nanzyo, M., Shoji, S., & Dahlgren, R. (1993). Volcanic ash soils: Genesis, properties and utilisation. In *Developments in Soil Science* (Vol. 21). Elsevier.

Ocampo-López, O. (2012). *Análisis de Vulnerabilidad de la Cuenca del río Chinchiná para condiciones estacionarias y de cambio climático* [Master's dissertation]. Universidad Nacional de Colombia, Manizales.

Otálvaro, D., Arias, G., Vélez, M., García, J., de la Rosa, P., Taupin, J., & Vargas, M. (2009). Plan de Manejo Integral del Agua Subterránea Modelo Hidrogeológico Conceptual Preliminar del Acuífero de Pereira, Colombia. *Estudios de Hidrología Isotópica En América Latina*, *2006*, 11–27.

Payne, B. R. (1992). On the statistical treatment of environmental isotope data in hydrology. In *Isotope techniques in water resources development*; 1991.

Peña, K. (2016). *Análisis de la variabilidad hidroclimática y dinámica glaciar en la cuenca alta de Río Claro (Villamaría Caldas, Colombia), Estudio científico como base para la adaptación y mitigación al cambio climático en la alta montaña colombiana*. Pontificia Universidad Javeriana.

Piña, A., Donado, L. D., Blake, S., & Cramer, T. (2018). Compositional multivariate statistical analysis of the hydrogeochemical processes in a fractured massif: La Línea tunnel project, Colombia. *Applied Geochemistry*, *95*, 1–18. https://doi.org/10.1016/j.apgeochem.2018.05.012

Podwojewski, P., Poulenard, J., Zambrana, T., & Hofstede, R. (2002). Overgrazing effects on vegetation cover and properties of volcanic ash soil in the páramo of Llangahua and La Esperanza (Tungurahua, Ecuador). *Soil Use and Management*, *18*, 45–55.

Poulenard, J., Podwojewski, P., & Herbillon, A. J. (2003). Characteristics of nonallophanic andisols with hydric properties from the Ecuadorian páramos. *Geoderma*, *117*, 267–281.

Poveda, G. (2004). La hidroclimatología de Colombia: una síntesis desde la escala inter-decadal hasta la escala diurna. *Revista de la Academia Colombiana de Ciencias*, *28*(107), 201–202.

Poveda, G., Waylen, P. R., & Pulwarty, R. S. (2006). Annual and inter-annual variability of the present climate in northern South America and southern Mesoamerica. *Palaeogeography, Palaeoclimatology, Palaeoecology*, *234*(1), 3–27. https://doi.org/10.1016/j.palaeo.2005.10.031

Rabatel, A., Ceballos, J. L., Micheletti, N., Jordan, E., Braitmeier, M., González, J., Mölg, N., Ménégoz, M., Huggel, M., & Zemp, M. (2018). Toward an imminent extinction of Colombian glaciers? *Geografiska Annaler. Series A: Physical Geography*, *100*(1), 75–95. https://doi.org/10.1080/04353676.2017.1383015

Ramón-Reinozo, M., Ballari, D., Cabrera, J. J., Crespo, P., & Carrillo-Rojas, G. (2019). Altitudinal and temporal evapotranspiration dynamics via remote sensing and vegetation index-based modelling over a scarce-monitored, high-altitudinal Andean páramo ecosystem of southern Ecuador. *Environmental Earth Sciences*, *78*(11), 1–15. https://doi.org/10.1007/s12665-019-8337-6

Rank, D., & Papesch, W. (2005). Isotopic composition of precipitation in Austria in relation to air circulation patterns and climate. In *Isotopic Composition of Precipitation in the Mediterranean Basin in Relation to Air Circulation Patterns and Climate*, 2000–2004. International Atomic Energy Agency (IAEA).

Risi, C., Bony, S., & Vimeux, F. (2008). Influence of convective processes on the isotopic composition ($\delta^{18}O$ and δD) of precipitation and water vapor in the tropics: 2. Physical interpretation of the amount effect. *Journal of Geophysical Research-Atmospheres*, *113*(19), 1–12. https://doi.org/10.1029/2008JD009943

Robertson, P. K., Flórez, A., & Ceballos, L. (2002). Volcanic geomorphology, activity and classification in Colombia. *Cuadernos de Geografía: Revista Colombiana de Geografía*, *11*(2), 37–76.

Rodríguez, C. (2004). Isotopic meteoric line for Colombia. *Meteorología Colombiana*, *8*, 43–51.

Rodríguez-Morales, M., Acevedo-Novoa, D., Machado, D., Ablan, M., Dugarte, W., & Dávila, F. (2019). Ecohydrology of the Venezuelan páramo: Water balance of a high Andean watershed. *Plant Ecology and Diversity*, *12*(6), 573–591. https://doi.org/10.1080/17550874.2019.1673494

Rousseaux, J. M., & Warkentin, B. P. (1976). Surface properties and forces holding water in allophane soils. *Soil Science Society of America Journal*, *40*, 446–451.

Rozanski, K., & Araguas-Araguas, L. (1995). Spatial and temporal variability of stable isotope composition of precipitation over the south American continent. *Bulletin: Institut Francais d'Etudes Andines*, *24*(3), 379–390.

Rozanski, K., Araguás-Araguás, L., & Gonfiantini, R. (1993). Isotopic patterns in modern global precipitation. *Climate Change in Continental Isotopic Records*, *78*, 1–36.

Ruiz-Vásquez, M., Arias, P. A., Martínez, J. A., & Espinoza, J. C. (2020). Effects of Amazon basin deforestation on regional atmospheric circulation and water vapor transport towards tropical South America. *Climate Dynamics*, *54*(9–10), 4169–4189. https://doi.org/10.1007/s00382-020-05223-4

Sakamoto, M. S., Ambrizzi, T., & Poveda, G. (2011). Moisture sources and life cycle of convective systems over Western Colombia. *Advances in Meteorology*, *2011*, 1–11. https://doi.org/10.1155/2011/890759

Samuels-Crow, K. E., Galewsky, J., Hardy, D. R., Sharp, Z. D., Worden, J., & Braun, C. (2014). Upwind convective influences on the isotopic composition of atmospheric water vapor over the tropical Andes. *Journal of Geophysical Research*, *119*(12), 7051–7063. https://doi.org/10.1002/2014JD021487

Sánchez-Murillo, R., Durán-Quesada, A. M., Birkel, C., Esquivel-Hernández, G., & Boll, J. (2017). Tropical precipitation anomalies and d-excess evolution during El Niño 2014-16. *Hydrological Processes*, *31*(4), 956–967. https://doi.org/10.1002/hyp.11088

Sarmiento, C., Cadena, C., Sarmiento, M., Zapata, J., & León, O. (2013). *Aportes a la conservación estratégica de los páramos de Colombia: actualización de la cartografía de los complejos de páramo a escala 1: 100.000*. Instituto de Investigación de Recursos Biológicos Alexander von Humboldt.

Saylor, J. E., Mora, A., Horton, B. K., & Nie, J. (2009). Controls on the isotopic composition of surface water and precipitation in the northern Andes, Colombian eastern cordillera. *Geochimica et Cosmochimica Acta*, *73*(23), 6999–7018. https://doi.org/10.1016/j.gca.2009.08.030

Shoji, S., & Fujiwara, Y. (1984). Active aluminum and iron in the humus horizons of andosols fromnortheastern Japan: Their forms, properties, and significance in clay weathering. *Soil Science*, *137*(4), 216–226.

Siegenthaler, U., & Oeschger, H. (1980). Correlation of 18O in precipitation with temperature and altitude. *Nature*, *285*(5763), 314–317. https://doi.org/10.1038/285314a0

Sklenar, P., Duskova, E., & Balslev, H. (2010). Tropical and temperate: Evolutionary history of Páramo Flora. *The Botanical Review*, *77*, 71–108.

Sprenger, M., Tetzlaff, D., Tunaley, C., Dick, J., & Soulsby, C. (2017). Evaporation fractionation in a peatland drainage network affects stream water isotope composition. *Water Resources Research*, *53*(1), 851–866. https://doi.org/10.1002/2016WR019258

Stewart, M. K., Cox, M., James, M., & Lyon, G. (1983). *Institute of nuclear sciences*. Institute of Nuclear Sciences.

Sturm, C., Hoffmann, G., & Langmann, B. (2007). Simulation of the stable water isotopes in precipitation over South America: Comparing regional to global circulation models. *Journal of Climate*, *20*, 3730–3750. https://doi.org/10.1175/JCLI4194.1

Tangarife-Escobar, A., Koeniger, P., López-Moreno, J. I., Botía, S., & Ceballos-Liévano, J. L. (2023). Spatio-temporal variability of stable isotopes in precipitation and stream water of a high elevation tropical catchment in the Central Andes of Colombia (version 1) [data set]. Zenodo. https://doi.org/10.5281/zenodo.7716975

Toro, L., Calderon, J., Taupin, J., & Vargas-Quintero, M. (2009). Exploración de las aguas subterráneas en Maicao (Colombia) mediante técnicas hidroquímicas e isotópicas. *Estudios de Hidrología Isotópica en América Latina*, *2006*, 67–82.

Valdivielso, S., Vázquez-Suñé, E., & Custodio, E. (2020). Origin and variability of oxygen and hydrogen isotopic composition of precipitation in the Central Andes: A review. *Journal of Hydrology*, *587*, 124899. https://doi.org/10.1016/j.jhydrol.2020.124899

Vallet-Coulomb, C., Gasse, F., & Sonzogni, C. (2008). Seasonal evolution of the isotopic composition of atmospheric water vapour above a tropical lake: Deuterium excess and implication for water recycling. *Geochimica et Cosmochimica Acta*, *72*, 4661–4674. https://doi.org/10.1016/j.gca.2008.06.025

van der Hammen, T., & Cleef, A. M. (1986). Development of the high Andean páramo flora and vegetation. In F. Vuilleumier & M. Monasterio (Eds.), *High altitude tropical biogeography* (pp. 153–201). Oxford University Press.

Villacis, M., Vimeux, F., & Taupin, J. (2008). Analysis of the climate controls on the isotopic composition of precipitation ($\delta^{18}O$) at nuevo Rocafuerte, 74.5° W, 0.9° S, 250 m, Ecuador. *Comptes Rendus Geoscience*, *340*, 1–9. https://doi.org/10.1016/j.crte.2007.11.003

Vimeux, F., Gallaire, R., Bony, S., Hoffmann, G., & Chiang, J. C. H. (2005). What are the climate controls on δD in precipitation in the Zongo Valley (Bolivia)? Implications for the Illimani ice core interpretation. *Earth and Planetary Science Letters*, *240*(2), 205–220. https://doi.org/10.1016/j.epsl.2005.09.031

Vimeux, F., Tremoy, G., Risi, C., & Gallaire, R. (2011). A strong control of the south American SeeSaw on the intra-seasonal variability of the

isotopic composition of precipitation in the Bolivian Andes. *Earth and Planetary Science Letters*, *307*(1–2), 47–58. https://doi.org/10.1016/j.epsl.2011.04.031

Vuille, M., Bradley, R. S., Werner, M., Healy, R., & Keimig, F. (2003). Modeling $\delta^{18}O$ in precipitation over the tropical Americas: 1. Interannual variability and climatic controls. *Journal of Geophysical Research-Atmospheres*, *108*(D6). https://doi.org/10.1029/2001jd002038

Vuille, M., Burns, S. J., Taylor, B. L., Cruz, F. W., Bird, B. W., Abbott, M. B., Kanner, L. C., Cheng, H., & Novello, V. F. (2012). A review of the south American monsoon history as recorded in stable isotopic proxies over the past two millennia. *Climate of the Past*, *8*, 1309–1321. https://doi.org/10.5194/cp-8-1309-2012

Vuille, M. (2018). Current state and future challenges in stable isotope applications of the tropical hydrologic cycle (invited commentary). *Hydrological Processes*, *32*(9), 1313–1317. https://doi.org/10.1002/hyp.11490

Vuille, M., & Werner, M. (2005). Stable isotopes in precipitation recording south American summer monsoon and ENSO variability: Observations and model results. *Climate Dynamics*, *25*(4), 401–413. https://doi.org/10.1007/s00382-005-0049-9

WGMS. (2017). In S. U. N. Zemp, I. Gärtner-Roer, J. Huber, H. Machguth, F. Paul, & M. Hoelzle (Eds.), *Global glacier change bulletin* (Vol. 2). ICSU (WDS)/IUGG(IACS)/UNEP/UNESCO/WMO.

Windhorst, D., Waltz, T., Timbe, E., Frede, H. G., & Breuer, L. (2013). Impact of elevation and weather patterns on the isotopic composition of precipitation in a tropical montane rainforest. *Hydrology and Earth System Sciences*, *17*(1), 409–419. https://doi.org/10.5194/hess-17-409-2013

Yang, J., Dudley, B. D., Montgomery, K., & Hodgetts, W. (2020). Characterizing spatial and temporal variation in ^{18}O and ^{2}H content of New Zealand river water for better understanding of hydrologic processes. *Hydrological Processes*, *34*(26), 5474–5488. https://doi.org/10.1002/hyp.13962

Zhang, J., Genty, D., Sirieix, C., Michel, S., Minster, B., & Régnier, E. (2020). Quantitative assessments of moisture sources and temperature governing rainfall $\delta^{18}O$ from 20 years' monitoring records in SW-France: Importance for isotopic-based climate reconstructions. *Journal of Hydrology*, *591*, 125327. https://doi.org/10.1016/j.jhydrol.2020.125327

SUPPORTING INFORMATION

Additional supporting information can be found online in the Supporting Information section at the end of this article.

How to cite this article: Tangarife-Escobar, A., Koeniger, P., López-Moreno, J. I., Botía, S., & Ceballos-Liévano, J. L. (2023). Spatiotemporal variability of stable isotopes in precipitation and stream water in a high elevation tropical catchment in the Central Andes of Colombia. *Hydrological Processes*, *37*(5), e14873. https://doi.org/10.1002/hyp.14873